ISTC PROJECT #B-070-98

JOINT INSTITUTE OF POWER AND NUCLEAR RESEARCH

NATIONAL ACADEMY OF SCIENCES OF BELARUS

MINSK, SOSNY

EXPERIMENTAL AND THEORETICAL RESEARCH OF THE PECULIARITIES OF TRANSMUTATION OF LONG-LIVED FISSION PRODUCTS AND MINOR-ACTINIDES IN SUB-CRITICAL ASSEMBLY DRIVEN BY A NEUTRON GENERATOR

Scientific leader **Dr. S.E. Chigrinov**

Project manager **I.G. Serafimovich**

1. Introduction

Investigations of high energy particles interaction with nuclei in spite of a great deal of experimental and theoretical issues are of great importance as before for study of peculiarities of nuclear reactions mechanism, atomic nucleus structure and elementary particles' physics. Further research in the field of nuclear physics fundamentals is still being stimulated by necessity of the solution of a wide range of applied problems, in particular the application of charged particles accelerators for energy production, transmutation of long-lived waste of fuel cycle of nuclear power engineering, tritium production, production of isotopes for industry, agriculture, medicine etc.

The problem of radioactive waste of nuclear power engineering management became recently especially important due to further extension of nuclear energy contribution to world energy production, setting up the nuclear power plants with inherent safety features eliminating all possibility of uncontrollable development of fission process and consequently accidental release of radioactive isotopes to environment and due to outstanding problems of open nuclear fuel cycle too.

One of the most prospective trends in solving the problem of long-lived radioactive fission products (^{137}Cs, ^{90}Sr, ^{129}I, Sn,...) and minor - actinides (Np, Pu, Cm ,…) amount reduction is transmutation that is its' conversion into stable or short-lived nuclei in sub-critical (target/blanket) systems driven by high energy charged particles accelerators (ADS - technology) [1-4]. The main advantage of ADS-technology is stable operation in sub-critical mode.

The concept of application of high energy accelerators is based on large-scale usage of high energy spallation reactions for neutron production in targets with A > 150 (Pb, Bi, W, U, Pb-Bi) with subsequent multiplication of generated neutrons in sub-critical blankets (k_{eff} ~ 0.9 - 0.98). In such systems high neutron flux densities ($\Phi \sim 10^{15}$-10^{17} n/(cm^2·s) can be achieved that is one of the main conditions for radioactive nuclides transmutation. Despite the considerable amount of theoretical researches the problem of choice of optimal neutron spectrum for transmutation of long-lived fission products - I, Cs, Sr, Zr and minor actinides - Np, Pu, Am, Cm remains by now one of the most important. It is connected mainly with lack of valid evaluated nuclear data on interactions of neutrons with radioactive nuclei (especially MA) in wide energy range (eV – GeV). For some nuclei even integral cross sections averaged over energy distributions are not available.

Principal aspects of ADS concept were widely discussed in theoretical papers but the experimental research in this field is rather scarce. As a rule the experiments on available high

energy particles' accelerators (LAMPF, AGS, ISR, JINR) are now being performed with the purpose of determination of neutron-producing targets characteristics (yields of neutrons, protons, isotopes production, spectra of neutrons escaping from targets). The experimental investigations at sub-critical systems are planned only because they are complicated, expensive and time consuming and often may not be realized with application of modern accelerators, since most of them have inappropriate beam parameters. In this regard the experimental research of various aspects of ADS on the basis of low energy accelerators – cyclotrons, microtrons, as well as deuterium and tritium ions accelerators representing neutron generators of high intensity is of great importance.

Application of such accelerators coupled with sub-critical multiplying systems ($k_{eff} < 1$) allows to carry out the experimental research of different aspects of ADS - technologies and to outline future investigations at high energy particle accelerators. Similar situation took place in nuclear power engineering when many peculiarities of neutron–physical characteristics of nuclear reactors, first of all of nuclear power plants cores intended for special purposes, were investigated at critical benchmarks.

The experimental research of physics of multiplying media with fast neutron spectra are being performed since 1995 in France (Cadarashe) at the sub-critical facility MASURCA, driven by neutron generator (E_n=14.1 MeV, I ~ 10^8 n/s). Core of MASURCA facility is loaded by MOX nuclear fuel ($UO_2 – PuO_2$ with relative Pu and U content (Pu/(U + Pu) = 34%). The program of research at MASURCA facility envisages measurements of both static and dynamic character [5].

First experimental investigations of ADS with thermal neutron spectrum at the National Academy of Sciences of Belarus were started in 2000 –2001 at the YALINA facility that is sub-critical assembly with polyethylene moderator and uranium dioxide fuel (10% enrichment by U-235) driven by neutron generator operating both in continuous and pulse modes. The results have shown that further investigations would be very prospective. The experiments at JINR (Russia, Dubna) accelerators performed in the framework of Program on Electronuclear Plants (# 03-01-1008-95/2005) [6] are the continuation of the investigation program as well as setting up booster sub-critical assembly driven by neutron generator that may be useful for working out the sub-critical assembly with fast neutron spectrum loaded by MOX fuel driven by proton (E_p = 660 MeV) accelerator (SAD facility, ISTC – Project) [7] and for TRADE -Project too [8].

2. Interaction of high energy radiation with matter

Interaction of high energy particles in energy range of some MeV - 10000 MeV is very complicated process involving participation of large number of heavy interacting particles (n, p, p-mesons) in which electromagnetic interactions, nuclear reactions, formation and development of nuclear cascade are taken into account. Transport of high energy radiation through dense media is accompanied mainly by two types of interactions: electromagnetic and nuclear ones. In process of interaction the charged particle loses part of its energy on excitation and ionization of atoms, Ozhe-electrons production or undergoes elastic scattering in the Coulomb field of nucleus. Main part of the energy losses occur due to ionization. This type of interaction has been studied experimentally and theoretically. Nuclear interaction results in new particles generation which number and characteristics depend on properties of primary particle initiating nuclear reaction. By movement in the matter high energy particle initiate the development of nucleon-meson cascade that is the process with participation of large number of particles. The extent of development of nucleon-meson or intra-nuclear cascade depends on medium characteristics, energy and type of primary particle. The development of intra-nuclear cascade attenuates as new particles generation with lower energy appears and finally results in scattering, moderation and absorption of neutrons. In fissionable media such chain of nuclear reactions includes fission of heavy nuclei by high energy particles and by neutrons of evaporation and fission spectra too.

It is obvious that time of interaction process can be divided into some stages that are defined by mechanism of the interaction, duration of nuclear reactions, peculiarities of transport of high and low energy particles through the matter and by properties of medium. Depending on type and energy of primary particle and on properties of matter one can speak about time from 10^{-21} s to millisecond and seconds for fissile media.

The calculation of such a complicated process can be performed in the frame of transport theory by neglecting quantum mechanical effects and by the following assumptions [9]:

- particles of nucleon-meson cascade are classical ones;
- wave-length of a particle is less than a distance between nuclei of substance;
- every moment of time t a particle interacts with one nucleus only;
- particles of nucleon-meson cascade do not interact each other.

By working out a balance equation of j-type particles number

$$dN_j = \Phi(r, E, \Omega) dr dE d\Omega$$

in phase space element dr dE dΩ at pointed above limitations the steady-state equations for transport of particles can be expressed.:

$$\hat{L}_j \Phi_j = Q_j + G_j \qquad (1)$$

at boundary conditions on convex surface S:

$$\Phi_j(r, E, \Omega) \mid_S = \Phi_{0j}(E, \Omega), \qquad \Omega \cdot n < 0, \qquad (2)$$

where n – is perpendicular to surface S near Ω;

$F_j(r,E,W)$ is differential flux density for j-type particles in a point r:

$$\hat{L}_j = \Omega\nabla + \sum\nolimits_j (r, E) + \sum\nolimits_{jD} (r, E) - \frac{\partial}{\partial E} b_j(r, E), \qquad (3)$$

$$Q_j = \sum_i \int d\Omega \int dE' \sum\nolimits_{ij}^{S} (r, E' \to E, \Omega' \to \Omega) \Phi_i(r, E', \Omega'), \qquad (4)$$

$$G_j = G_j(r, E, \Omega). \qquad (5)$$

and G_j is intensity of external source.

The terms of equation (3) define main processes involved in nucleon-meson cascade development: leakage of particles from elementary volume ***dr*** by fixed values of ***E*** and ***O***; losses of particles as a result of interaction with atom nuclei; decay of unstable particles; continuous losses of energy by charged particles as a result of electro-magnetic interactions with transmission of small portions of energy (continuous slowing). The equations (4) and (5) define the formation (increasing) of particles number due to elastic or non-elastic scattering when particle of i-type with coordinates ***E'*** and ***O'*** in phase space in the neighborhood of point ***r*** forms particle of j-type in energy interval ***dE*** near ***E***, in direction interval ***dO*** near ***O*** (in particular case $i = j$) and source directly emitting particles of j-type in pointed element of phase space.

Differential cross-section of inclusive reaction is equal

$$i + A \to j + X \qquad (6)$$

$$\sum\nolimits_{ij}^{S} (r, E' \to E, m_S) = \frac{n(r)}{r(r)} p_j f_{ij}(r, p_j, S), \qquad (7)$$

where $f_{ij} = Ed^3s/d^3p$ is single-particle invariant differential cross-section. When writing time-dependent transport equations the item should be added to the left part of the equation (1):

$$\frac{1}{n} \frac{\partial}{\partial t} \Phi_j(r, E, \Omega, t), \qquad (8)$$

where v is the velocity of j-type particle.

Analytical description of such a complicated process on the basis of solution of kinetic equations set (1) and (2) for flux densities of various particles (n, p, $\bar{p}$, p^0, p^+, $^-$, e^+, γ,..) is

possible only by simplifying the solution assumptions both of mathematical and physical character and obviously for simple geometries. Correct description of high energy particle interaction with matter can be performed by means of Monte Carlo method which statistical approach more adequately reflects the physics of phenomenon and is most suitable instrument to take into account all details of nuclear reaction mechanism and particle transport both in high and low energy range. The central point of calculation of high energy particles interaction with matter is correct description of multiple generation of hadrons in the reactions of inelastic collision of high energy particles and nuclei with medium nuclei. For this purpose phenomenological inclusive distributions are used (7) or exclusive approach that gives more detail information about properties of secondary particles born in inelastic collisions.

In the process of transport of high energy particles and nuclei through various media two stages can be distinguished differing by duration, character of interaction and type of secondary particles. The first stage is characterized by intense generation of secondary particles (n, p, π, γ) in high energy reactions of spallation and fission, particles' transportation in substance finished by production of neutrons with energy $E_n \leq$ 10-20 MeV. The second stage involves transport of low energy neutrons. It means that the problem of calculation of intra-nuclear cascade can be turned to determination of the characteristics of low energy neutrons source (its energy, space and angle distributions) with subsequent calculation of neutrons transport based on transport theory methods and on nuclear reactors theory for fissionable media.

By solving particles transport equations (1) it is necessary to define type of function (7) determining basic characteristics of the particles formed in inelastic nuclear interactions. Most prospective is the approach based on models developed in relativistic nuclear physics.

Nuclear reactions in high energy range are described correctly in the frame of cascade-exciton model interpreting the interaction of particles with nuclei as three stages process: cascade, pre-equilibrium and equilibrium stages. Characteristic energy ranges corresponding to the stages of nuclear reaction can be distinguished in the energy spectrum of secondary neutrons. For example, equilibrium stage is responsible mainly for generation of low energy neutrons ($E_n <$ 20 MeV). In particular, it can be written for inclusive spectrum of the particles formed in inelastic reactions [10]:

$$s(p)dp = s_{in}[N^{cas}(p) + N^{prq}(p) + N^{eq}(p)]dp\,, \qquad (9)$$

where $N^{cas}(p)$, $N^{prq}(p)$ and $N^{eq}(p)$ are cascade, pre-equilibrium and equilibrium components of spectrum.

Spectrum of particles formed at cascade stage can be written as:

$$N^{cas}(p)\cdot dp = [\int_0 d^2b \int_{r>R}^{R} dr \int_0^{t^{cas}} dt\, f^{cas}(r,p,t)dp]/s_{in}, \qquad (10)$$

where $f^{cas}(r,p,t)$ is function of distribution of cascade particles and b – aiming parameter of collisions of particles escaped from a nucleus with radius R at the end of cascade stage t_{casc}.

To determine $N^{cas}(p)dp$ Monte Carlo method is used. Its statistical nature allows more adequately take into account all the peculiarities of cascade mechanism of nuclear reaction treating the interaction of high energy particles with nucleus as sequence of quasi-free collisions of cascade particles with inter-nuclear nucleons. It means that in energy range $E >> E_f + (1,2)$ $E_b + V_c$, where E_f – Fermi energy, E_b – binding energy, and V_c - Coulomb barrier, energy and angle distributions of secondary particles will be defined mainly by the characteristics of p-N- and N-N-collisions.

Second term of the equation (9) represents contribution of pre-equilibrium stage of nuclear reaction describing de-excitation process of the non-equilibrium nuclear system after completion of cascade stage of the reaction. In this part of the reaction energy spectrum of secondary particles is defined only by density of the excitons' states $n = p + h$ and second power of matrix transition between stages with different numbers of excitons. Pre-equilibrium component in inclusive spectrum of the particles is presented as [10]:

$$N^{prq}(p)dp = \int_{t^{cas}}^{t^{eq}} dt \sum_{n,E} l_c^j(n,E,T)P(n,E,t)\cdot \partial(p\Omega)/\partial(t,\Omega)\cdot F(\Omega)dTd\Omega, \qquad (11)$$

where $l_c^J(n,E,T)$ is a probability of j-type particle emission in energy range T, $T+dT$ from the state with n excitons at moment t; $P(n,E,t)$ is a probability to find out excited nucleus at time t after cascade stage in state with exciton number $n = p + h$ and energy E, where p and h are the hole and particles numbers, respectively.

Function $P(n,E,t)$ is defined by proper kinetic equation including the transitions Dn = -2, 0 and +2, and probability of emission of a particle into continuous spectrum $\Gamma_j(n,E)$:

$$\Gamma_j(n,E) = \int_{V_j}^{E-B_j} l_c^j(n,E,T)dT; \qquad (12)$$

$$l_c^j(n,E,T) = (2S_j+1)/(p^2h^3)\, m_j R_j(n)\, w(n',E-B_j-T)/w(n,E)\, T\, s_{inv}(T),$$

where S_j is spin, B_j – binding energy, V_j - Coulomb barrier, m_j – reduced mass of evaporated particle, n - exciton number. Factor $R_j(n)$ defines type j of a particle evaporated at pre-equilibrium stage from the state with n excitons.

It should be noted that main feature of the pre-equilibrium component is weak rise of its contribution by passing to heavy nuclei and independence of the shape of mass number pre-equilibrium spectrum. After the equilibrium state is achieved *(n ³ n_{eq})* when states with different exciton number have the same probabilities, the probability to radiate a particle is expressed as:

$$N^{eq}(p)dp = \int_{t_{eq}}^{\infty} dt \sum l_c^j(n,E,T)\cdot P(n,E,T)\cdot \partial(P,\Omega)/\partial(t,\Omega)\cdot d\Omega. \qquad (13)$$

Taken over *n* sum of the excited states density *W(E) = å w(n,E)* decreases as exponential curve *w (E) ~ exp(- 2ÖgE)* and at *t ³ t_{eq} (n>n_{eq})* traditional "evaporation" approximation may be used substituting in (7) *w(p,h,E) ® w(E) ~ exp 2Öa E* with level density parameter *a*= (1/10÷1/20)A MeV^{-1}. It follows from the equations describing nuclear reaction that shape of the differential energy distributions of particles formed in nuclear reactions in high energy range weakly depends upon type of projectile particles, its' energy and mass of target nucleus. In process of 14 MeV neutrons interaction it is possible to mark out also pre-equilibrium (fast) and equilibrium stages. In this case it should be expected too that distribution *dN/dE* will be the same as in high energy range. Let us consider for illustration the reaction of inelastic scattering *(n,n')* on Ta nucleus. As it seen from comparison of experimentally measured neutron spectrum and calculated one (Fig.1), in the frame of such reaction mechanism the general form of secondary neutron energy distribution is well reproduced.

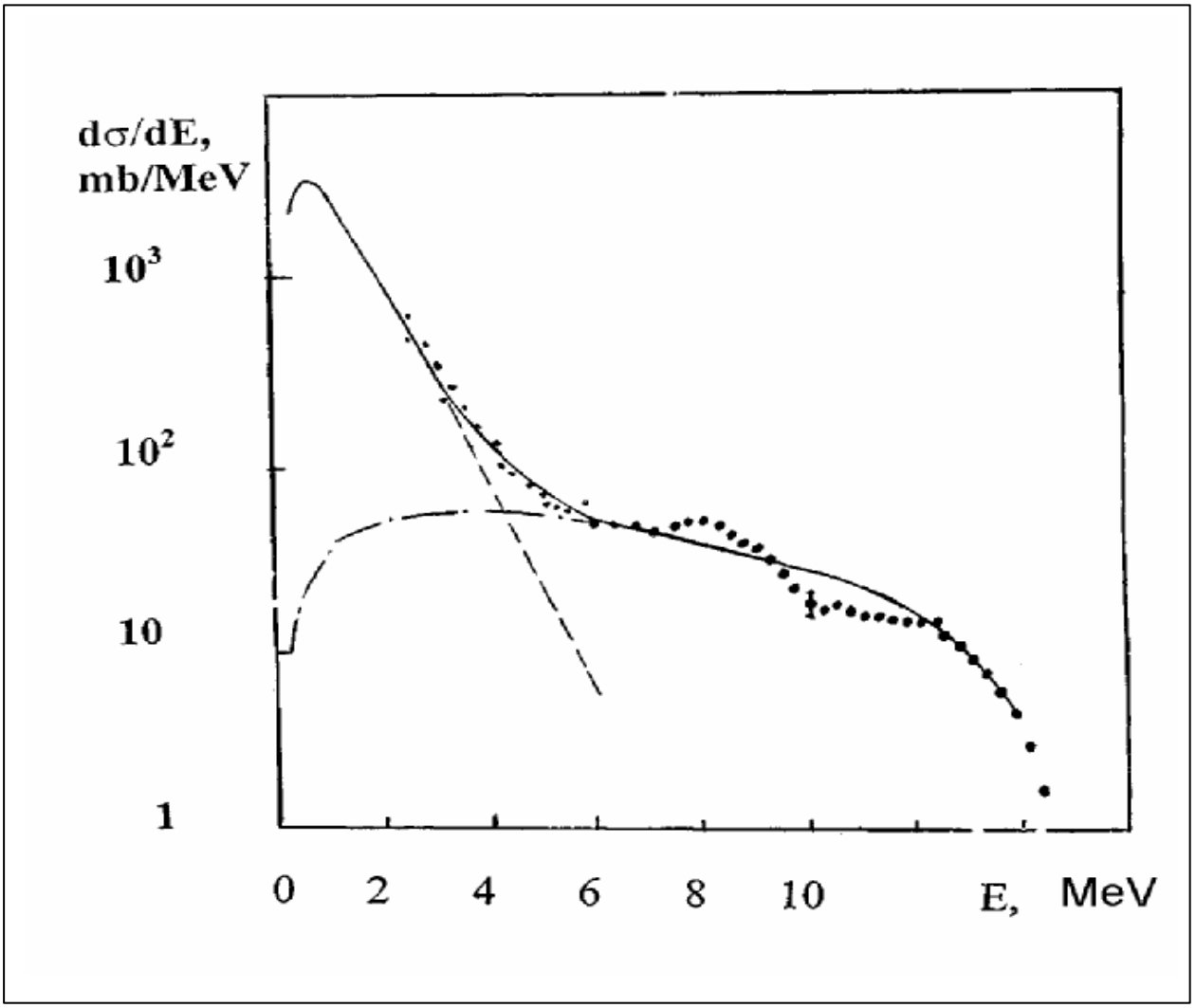

Fig. 1. Energy spectrum of neutrons, formed by interaction of neutrons with energy E_n = 14.1 MeV with Ta nuclei:

●●●●●●● - experimental data [11];

- - - - - - - evaporation component;

-●-●-●-●- - pre-equilibrium component;

_____ - total spectrum.

Pre-equilibrium component makes up about 25% and its contribution by T > 6 MeV becomes definitive. The contribution of pre-equilibrium stage of the reaction is well demonstrated by comparison of theoretical and experimental energy spectra of charged particles.

In Fig.2 proton spectra in reaction p + Fe → n + X+… for E_p =39 MeV are presented. One can see that main contribution to neutron energy spectrum make neutrons generated at final, evaporation stage.

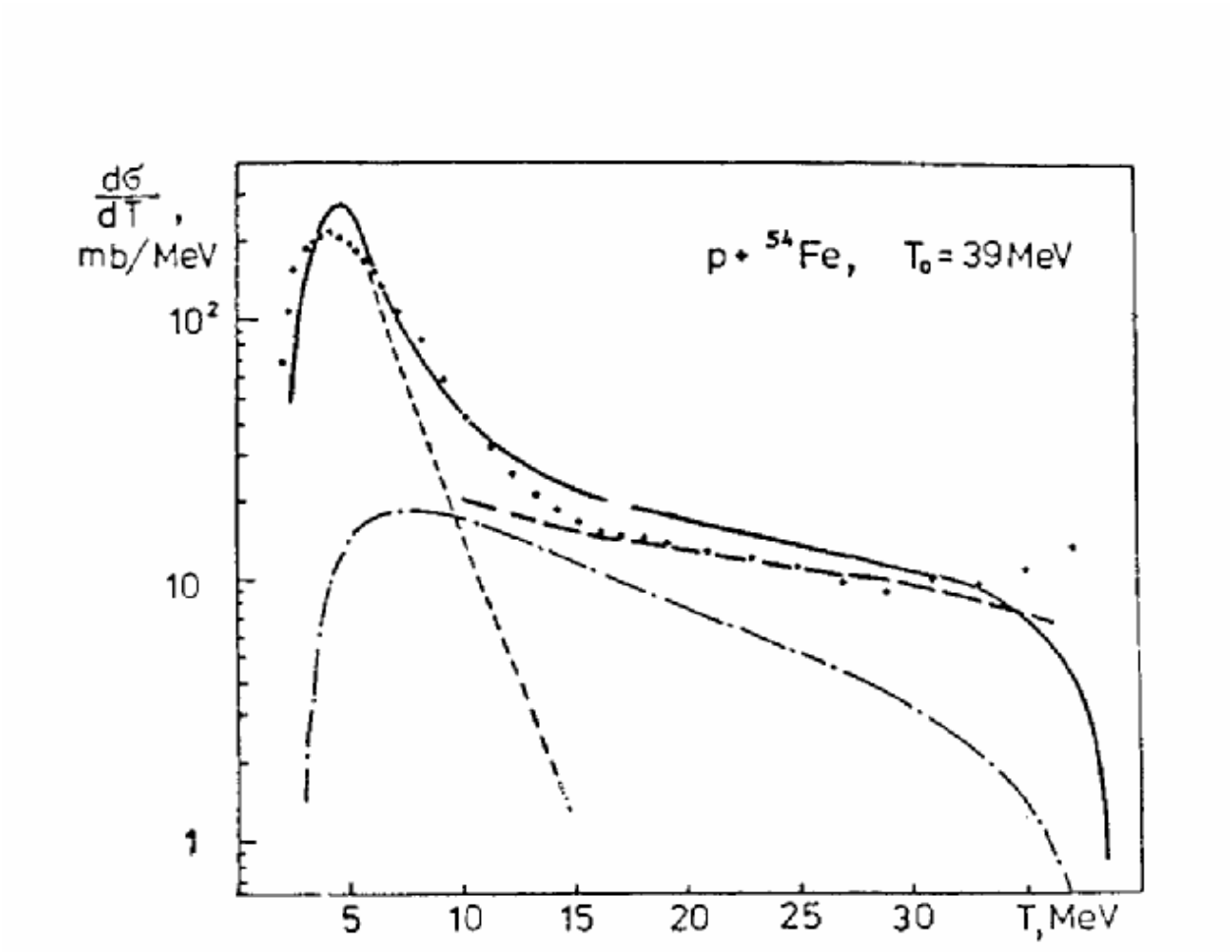

Fig.2. Energy spectrum of protons generated by interaction of protons with energy E_p =39 MeV with ^{54}Fe-nucleus.

●●●●●●● - experimental data [12];

- - - - - - - evaporation component;

-●-●-●-●- - pre-equilibrium component;

_____ - total spectrum.

In Fig.3 spectra of protons escaping from a target at various angles in neutron-- nucleus reactions by E_n =425 MeV are presented. In this case main contribution make protons formed at slow stage of the reaction. It should be noted that shape of distribution $d^2s/dEdW$ does not depend upon angle of particle emission from nucleus too.

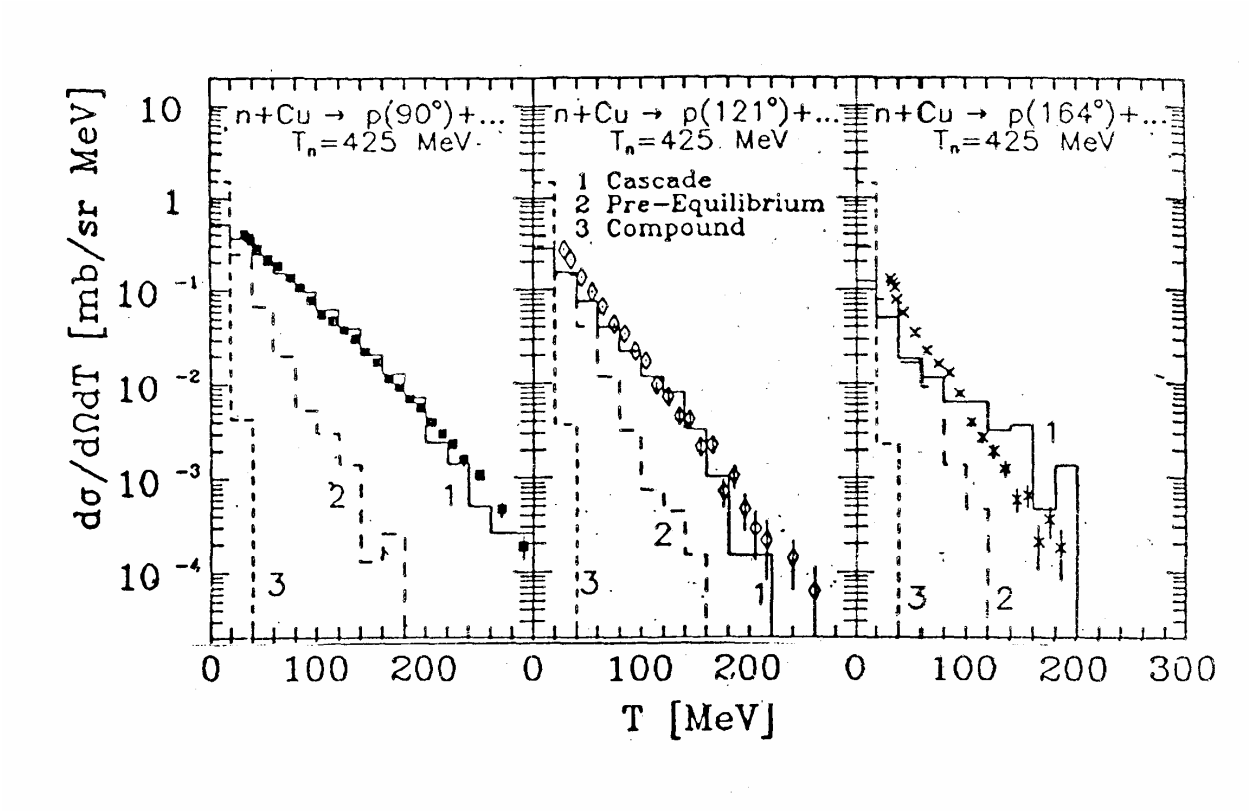

Fig. 3. Inclusive proton spectra in reactions n+ ^{69}Cu → p + X by E_n = 425 MeV at angles 90°, 121°, 164° [13]:

●●●●●● - experimental data;
- - - - - - cascade component;
- - - - - - pre-equilibrium component;
- - - - - - evaporation component.

As it was noted before transport of high energy particles and nuclei through a matter initiates development of nucleon-meson cascade. Neutrons formed in series of inelastic collisions of fast particles with target nuclei are predominant component of the cascade. As it was proved by theoretical and experimental researches main part of spectrum of neutrons emitted from neutron-producing lead target of ADS constitute neutrons in the energy range E < 15 – 20 MeV. By irradiation of the targets containing fissionable nuclei (Th, U, Pu, ...) a substantial contribution to neutron component in the energy range of 1-2 MeV will be made by neutrons generated in fission reactions so the energy distribution of neutron flux density will be undoubtedly defined by material composition of a medium. Obviously, a fraction of high energy particles will decrease as a target size increases due to reduction of the number of both elastic and inelastic interactions and spectrum of neutrons escaping from heavy targets will be defined first of all by neutrons with energies in the range of E_n < 15-20 MeV that are being formed mainly at slow evaporation stage of nuclear reaction. It should be noted that coming from the mechanism of pre-equilibrium and cascade stages of nuclear reactions that are defined by

properties of two-particles N-N and π-N interactions one should expect that in the energy range corresponding to these stages of reactions 15 MeV ≤ E ≤ 70 MeV spectra will be identical too.

So far as it was mentioned above main contribution to neutron spectrum in inelastic reactions initiated by 14 MeV neutrons makes evaporation stage too, one should expect that leakage spectra from extended targets made of W, Pb, Th, Bi, U,… irradiated by neutrons formed in $D + {}^3H \rightarrow {}^4He + n$ reactions or by high energy protons ($E_p \approx 0.8 - 2.0$ GeV), will be the same in the energy range of E_n < 15-20 MeV. It results in independence of neutron spectra upon a type of projectile particle and material of a target. In this connection the distribution of neutrons with E_n < 15-20 MeV escaped from the targets will be identical both for 14 MeV neutrons and for protons with energy about some GeV:

$$F(Ei) = \frac{1}{N_{sp}} \frac{1}{E_i / E_p} \frac{dN_i}{dE_i / E_p}, \qquad (14)$$

where E_i is energy of neutrons escaping from extended targets;

E_p is energy of projectile particle;

N_{sp} – number of neutrons escaping from a target with energy E_n < 15-20 MeV.

That it is really so is seen from Fig. 4-6 where experimental and theoretical spectra for neutrons escaping at angles $\theta = 50^0$ and $\theta = 130^0$ from uranium target (D=15 cm, L=30 cm) irradiated by 750 MeV protons as well as spectra of neutrons escaped from lead target (15 × 15 × 20cm) irradiated by protons with energies E_p=500 MeV, E_p=1500 MeV and neutrons with energy E_n =14.1 MeV at angles $15^0 < \theta < 150^0$ are presented.

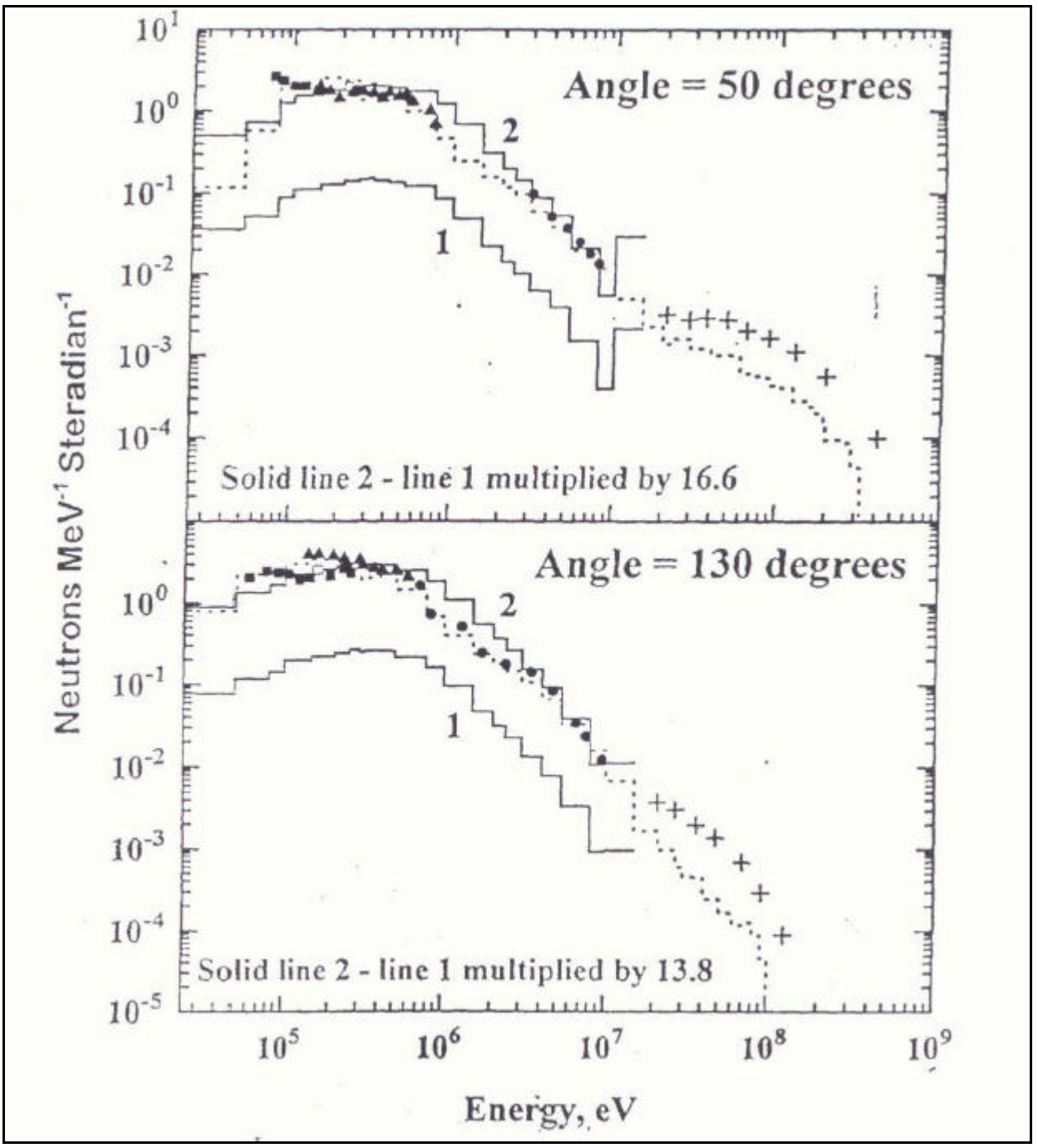

Fig.4. Comparison of the experimental and calculated spectra of neutrons escaping at angles θ=50° and θ=130° from uranium target with diameter D=15 cm and length L=30 cm irradiated by protons with energy E_p =750 MeV and neutrons with energy E_n =14.1 MeV. Histograms represent results of calculations with application of computer code LAHET [14], points are the experimental data [15]. Normalization factor for histogram 2 is - per one proton with energy 750 MeV, for histogram 1 – per one neutron with energy 14.1 MeV. Normalization for curve 2 was taken by energies 162 and 219 keV, respectively.

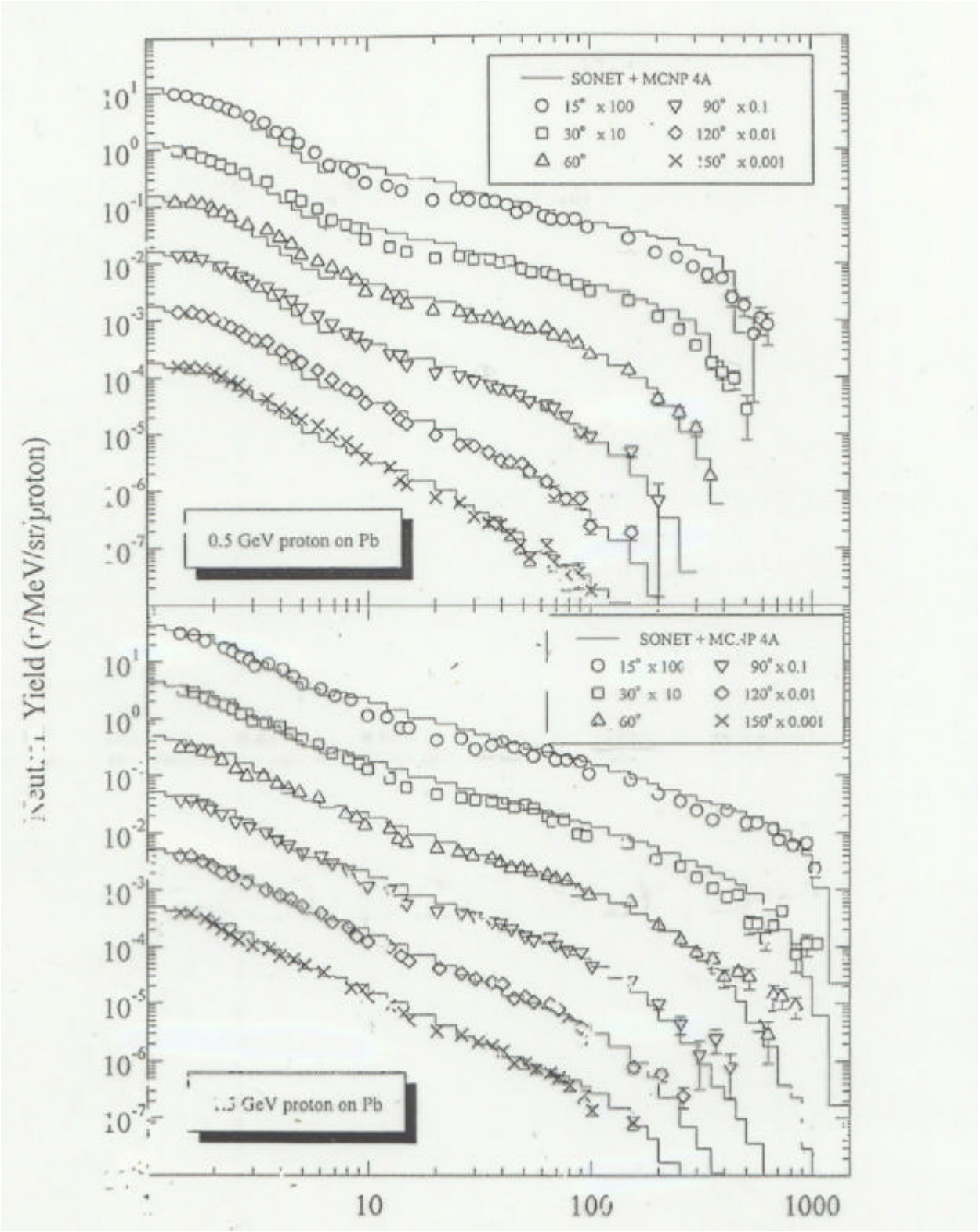

Fig.5. Experimental and calculated energy spectra of neutrons generated in lead target ($15\times15\times20$ cm^3) irradiated by protons with energies 500 and 1500 MeV [16]

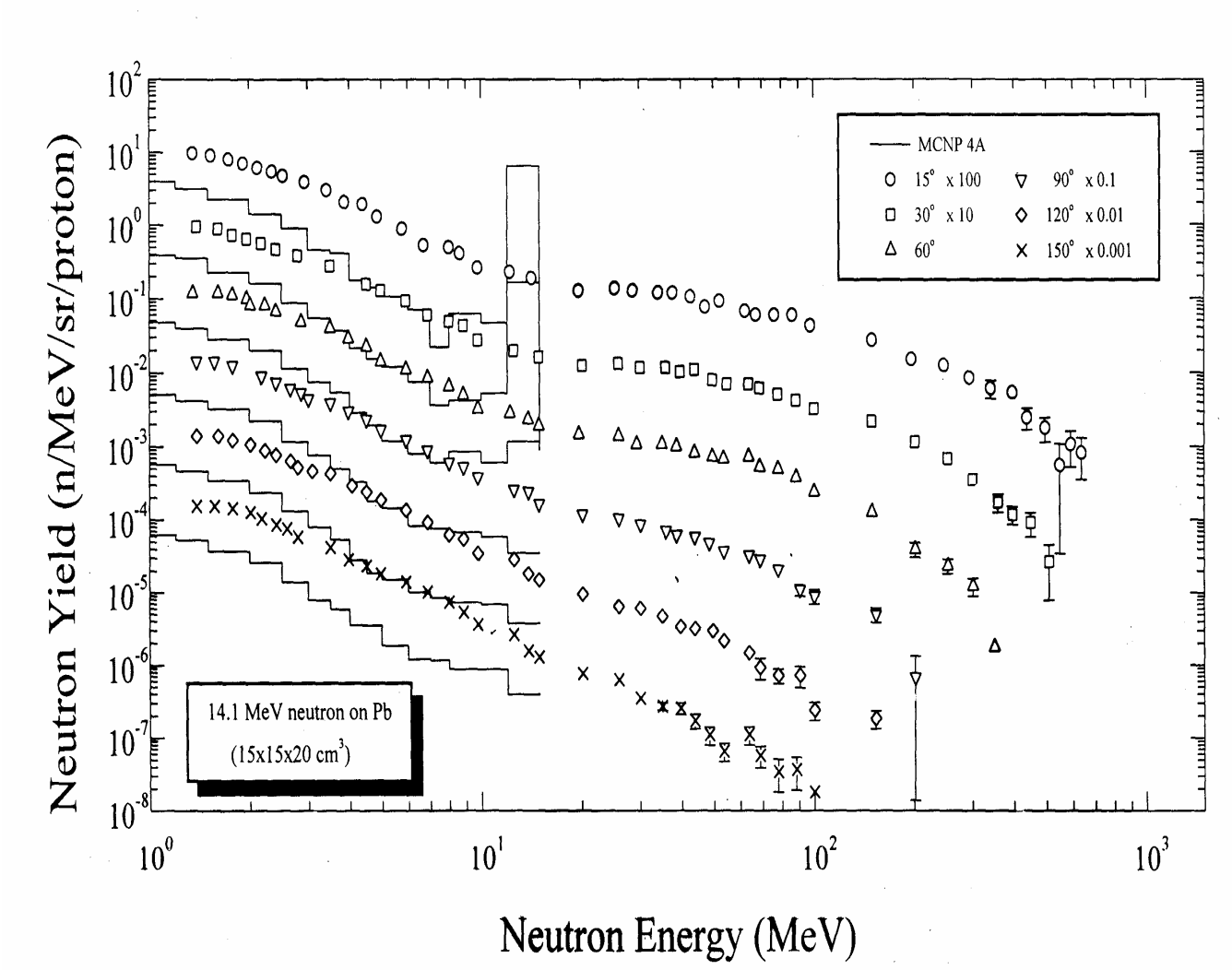

Experimental and calculated leakage neutron energy spectrum from a thick lead target of 15 by 15 cm in width and 20 cm in length bombarded with 14.1 MeV neutrons. The histograms indicate calculated results obtained with MCNP 4A. The symbols indicate experimental data taken from the paper by H. Takada et. al. in IAEA-TECDOC-985, 1997.

Fig.6. Experimental and calculated leakage neutron energy spectrum from a thick lead target of 15 cm in width and 20 cm in length bombarded by 14.1 MeV neutrons. The histograms demonstrate the results calculated by MCNP-4A code. The symbols indicate experimental data taken from the paper by H. Takada et. al. [16].

As it follows from presented data main contribution to $d^2s/dEdW$ make neutrons of low energies ($E_n \leq$ 15-20 MeV) which energy distribution is close to "evaporation" spectrum in contrast to high energy part that is formed due to the cascade and pre-equilibrium stages. It is obvious that fraction of cascade particles is defined by target dimension and will decrease with dimension increasing. Similarity of $d^2s/dWdE$ distributions in the energy range $E_n \leq$ 15-20 MeV provides a principal possibility of application of proton $E_p \leq$ 100-150 MeV, deuterium ions accelerators where main contribution to nucleon cascade makes reaction d + A $\rightarrow$ n + ... and electron accelerators (microtrons) in which spallation neutrons source is formed due to photo-spallation reactions γ + A$\rightarrow$ n+ X for investigations in the field of ADS-technology.

One more evidence of independence of the energy distribution of neutrons generated in spallation reactions in extended targets of heavy elements Pb, Bi, Th, U upon energy of primary proton beam are the results of experimental investigations of ^{129}I, ^{237}Np transmutation by relativistic protons ($0.5 < E_p < 7.4$ GeV) that have been carried out at the Laboratory of High Energies (LHE) of JINR (Dubna, Russia). It was determined that transmutation rates of ^{129}I(n,γ)^{130}I and ^{237}Np(n,γ)^{238}Np related to one neutron generated in neutron-producing Pb target do not depend upon energy of protons.

Just these considerations became a basic argument for setting up the nuclear sub-critical facility YALINA intended for carrying out the experimental investigation of physics of sub-critical systems with external neutron sources. The facility consists of sub-critical assembly driven by a neutron generator operating both in continuous and pulse modes.

The program of experimental investigations at the YALINA facility covers a wide range of problems dealing with physics of sub-critical systems driven by external neutron sources. In particular it includes development and check of the experimental methods of sub-criticality level measurement based on the methods worked out for critical systems, verification of the codes and nuclear data libraries, estimation of factors of neutron-producing target coupling with core, relative importance of external neutron source etc. The description of sub-critical assembly YALINA design with various core configurations, main parameters of the facility; experimental results obtained at the facility and comparison of calculated and experimental results will be presented below.

3. Sub-critical assembly YALINA with thermal neutron spectrum driven by a neutron generator.

Efforts on setting up the experimental facility with thermal neutron spectrum consisting of sub-critical target/blanket system driven by neutron generator of high intensity were started in 1998. Experimental investigations of neutronics of sub-critical systems driven by external neutron sources (neutrons of Cf-252 spontaneous fission spectrum, neutrons from reactions d(D,n)^{3}He and d(T,n)^{3}He) were started in 2001 after putting into operation the sub-critical assembly and deuterium ions accelerator operating both in continuous and pulse modes.

According to generally accepted principles of ADS-technology [1, 4, 5, 6, 7, 8, 16-19] the experimental facility consists of deuterium ions accelerator with Ti ^{3}H or Ti ^{2}H targets (neutron generator), sub-critical assembly loaded by uranium dioxide (10% of U-235), polyethylene moderator and Pb neutron-producing target, irradiated by neutrons with energy 14.1 or 2.5 MeV (Fig.7).

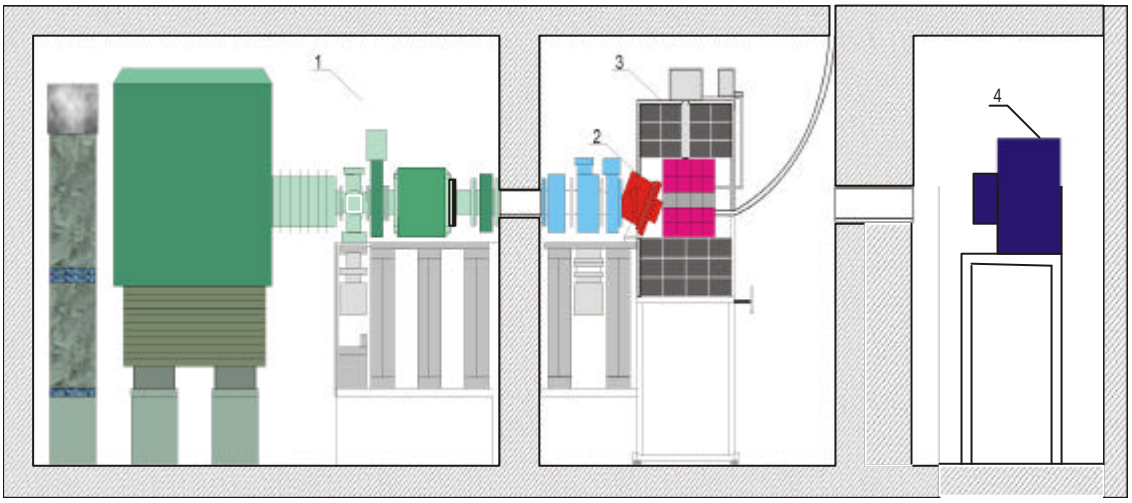

Fig. 7. Sub-critical facility YALINA: 1 –neutron generator; 2 - Ti^{3}H (TiD) target system; 3 sub-critical assembly, gamma-spectrometer.

The sub-critical assembly of YALINA facility is uranium - polyethylene multiplying system with $k_{max} < 0.98$, located inside graphite reflector of parallelepiped configuration with side dimension 1000 and 1200 mm that is arranged of high purity “reactor graphite” blocks with side dimension 200×200×500 mm. The core of the assembly is of parallelepiped configuration too with side dimension 400×400×600 mm and consists of “bare” polyethylene sub-assemblies where fuel rods of EK-10 type (UO_2 of 10% enrichment by U-235) are located. On the whole fuel subassembly contains 9 blocks (in height) made of polyethylene (γ

= 0.927 g/cm^3) with side dimension 80×80×63 mm and 16 fuel rods of EK-10 – type located in channels with diameter D = 11 mm (Fig.9). Fuel rods' spacing equal 20 mm is close to the optimal value for multiplying medium with polyethylene moderator and fuel rods EK-10.

Main considerations of moderator material choice were connected both with its moderating capabilities and availability. Among available at JIPNR moderating materials $ZrH_{1,8}$ and polyethylene seems to be preferable for sub-critical assembly with thermal neutron spectrum due to its' high moderating capability $\xi\Sigma_s$, moderating ratio $\xi\Sigma_s \Sigma_a^{-1}$ (Σ_s – neutron scattering cross-section, ξ- average logarithmic decrement of energy). Sub-critical systems with $ZrH_{1,8}$ – moderator are of special interest because $ZrH_{1,8}$ has high radiation and thermal stability, allows to get critical load in a small volume and to achieve high levels of specific power density. It allows to operate at high working temperatures (300-500°C), that is important for investigation of temperature reactivity effects, other reactivity effect components, sub-critical systems behavior in transient processes and so on. For the YALINA core polyethylene was chosen as moderator because of it's high moderating capability ($\xi\Sigma_s$ in the energy range of 1eV-100 keV is about 3.26, moderating ratio $\xi\Sigma_s \Sigma_a^{-1}$ =122), simplicity of handling that allows to create compact sub-critical assembly for investigation both of multiplying media physics and peculiarities of transmutation of radiotoxic waste of fuel cycle in the frame of ADS technology with thermal neutron spectrum.

At the core center a neutron-producing Pb target is located made of 12 blocks (in height) with side dimension 80×80×50 mm that reminds fuel subassembly by shape and size. Graphite reflector (thickness about 500 mm) is covered from outside by Cd – layer with thickness – 1mm. At the distances r = 50 mm, 100 mm, 150 mm from the core center three experimental channels with diameter D = 25 mm are situated for location of samples of radioactive targets and various detectors for measurement of neutron flux density functionals. For the same purpose two axial channels with diameters 25 mm are located in graphite reflector at the distances 250 mm and 358 mm; by z = h/2 one more radial channel with diameter 25 mm is located. As a whole, core of the sub-critical assembly contains 20 fuel subassemblies, 4 control rod subassemblies and Pb target of the same shape as fuel subassembly. Layout of the sub-critical assembly is presented in Fig.8, general view of the fuel subassembly – in Fig. 9, vertical (X-Y) section - in Fig. 10.

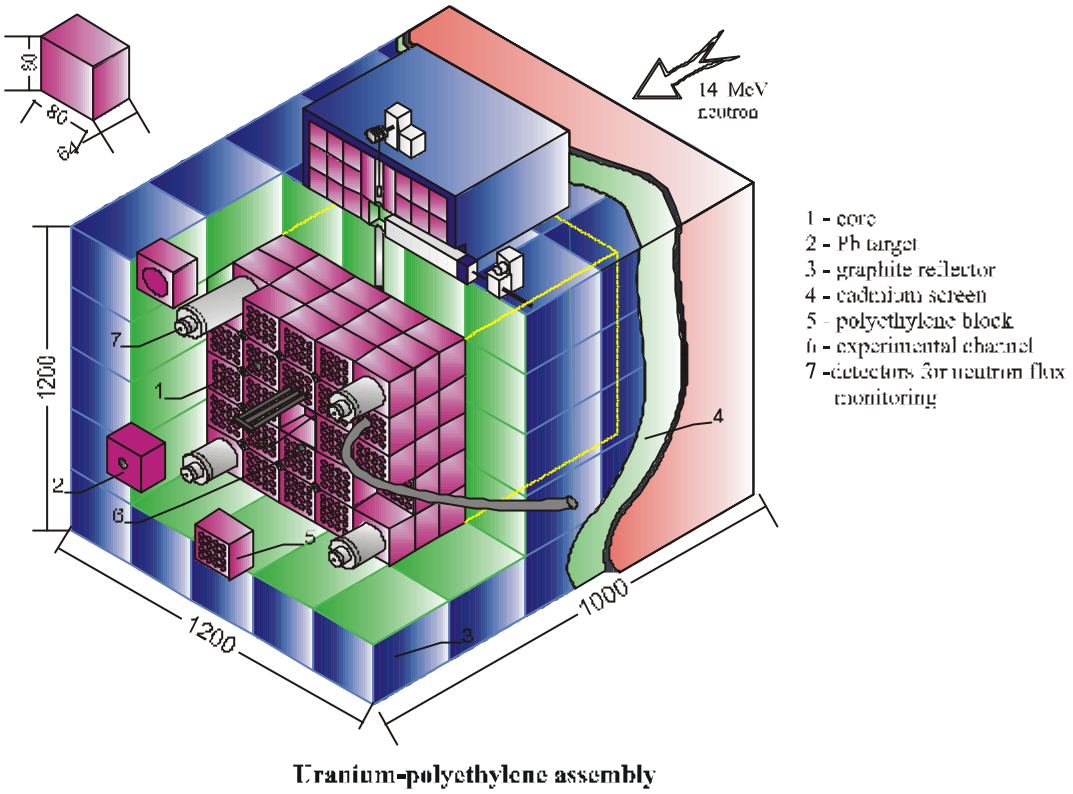

Fig.8. Layout of the sub-critical assembly.

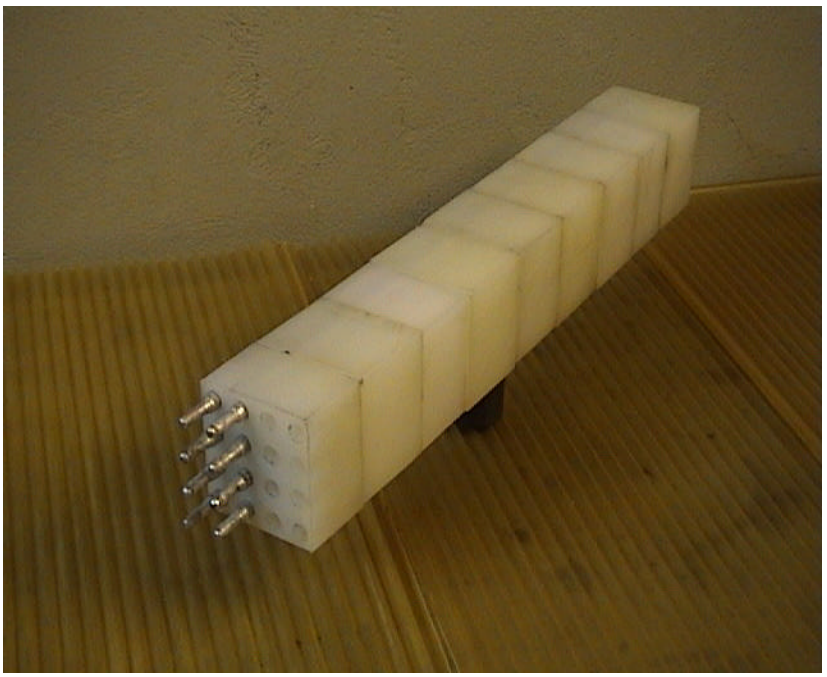

Fig. 9. General view of the YALINA fuel subassembly.

Parameters of sub-critical multiplying system (blanket) were chosen to provide:

- Inherent nuclear safety based on the assembly structure, technology of operation, control and maintenance methods;
- Maximum level of neutron flux density in experimental channels ($\Phi \approx 10^{7\text{-}8}$ n/(cm^2 s));
- Possibility of carrying out measurements inside core and reflector;
- Possibility of core rearrangement with the purpose of neutron flux density optimization in the points of irradiated targets and detectors location;
- Possibility of core design changes: insertion into the core zones with different fuel enrichments to cause changes of neutron spectrum in certain element of core volume, multiplication factor changes and so on;
- Possibility of external source location both inside and outside the core, that is creation of various configurations of the system «neutron source – sub-critical assembly»;
- Possibility of investigation of kinetic parameters of sub-critical multiplying media by wide variation of pulse duration and pulse repetition frequency of external neutron source;
- Experimental channels dimension necessary for location of various detectors, converters and so on;
- Wide possibilities for carrying out the experiments under condition of constant neutron flux densities in irradiated targets;
- Experimental channels should be located in such a way to be able to take into account all the peculiarities of ADS and minimize the influence of channels each other.

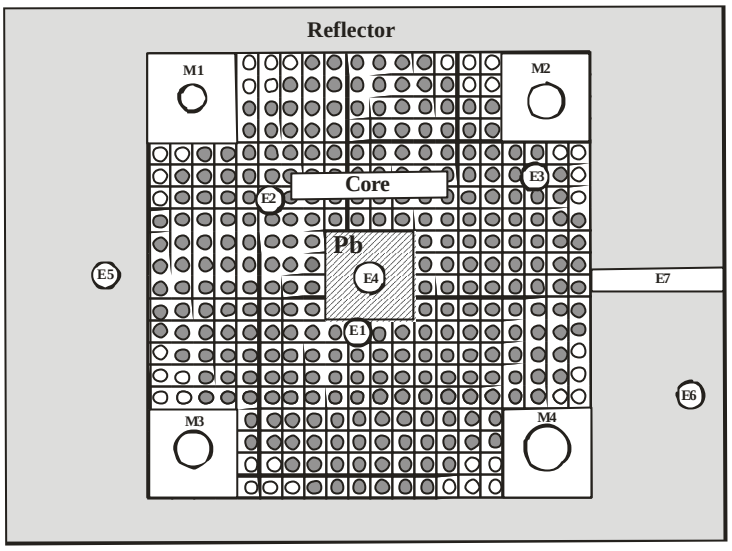

Uranium-polyethylene subcritical assembly

C - cross-section (280 fuel rods)
E1 -E 7, M1 - M 4 - experimental channels

Fig.10. Core configuration of the sub-critical assembly with fuel rod number N_p=280. E1-E3 – experimental channels inside the core; M1-M4 – channels for neutron flux monitoring; E5-E7 – experimental channels in reflector; E4 – channel in Pb - target.

One of the core configurations was intended for experiments on determination of lead zone influence on core parameters. Layout of this core configuration is presented in Fig.11.

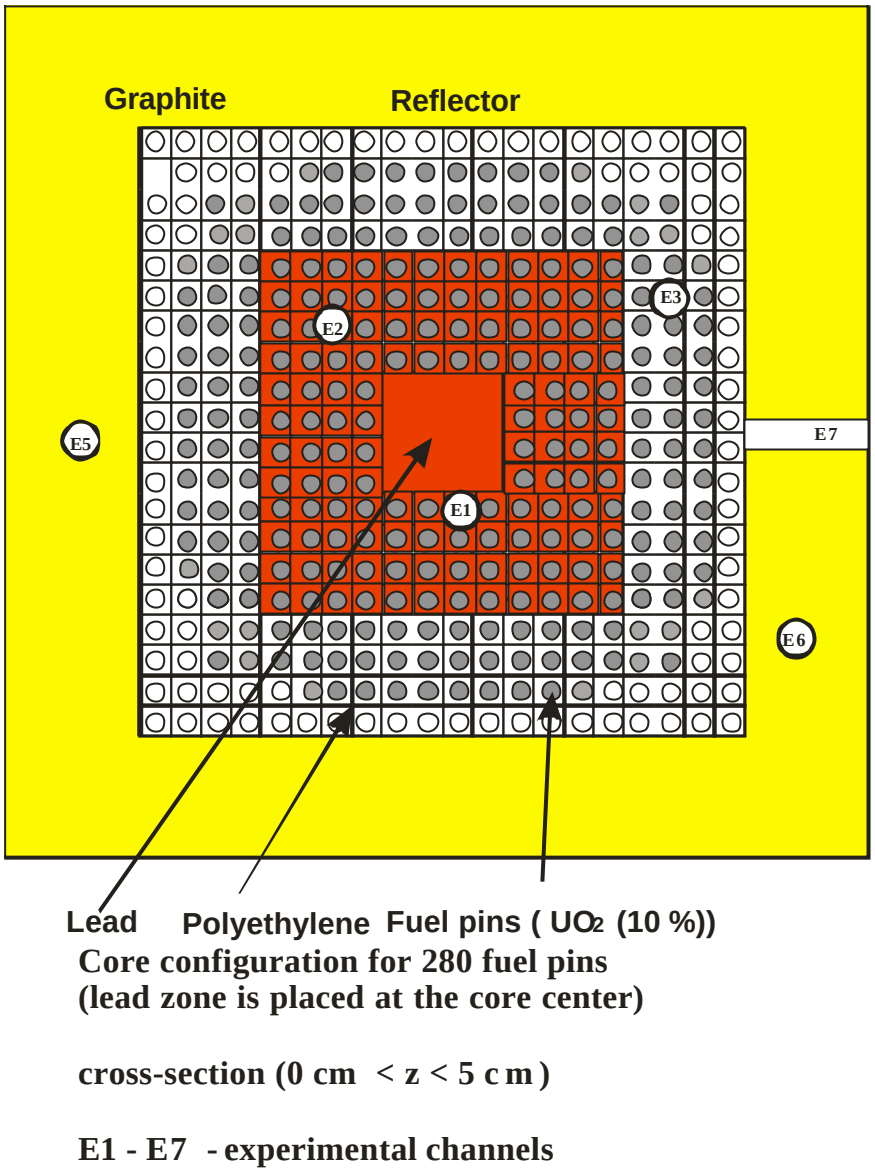

Fig.11. Layout of the core configuration with lead zone.

In this case deuterium and tritium targets are located at the center of lead zone, simulating presence of spallation neutrons source at blanket. Investigation of neutronics peculiarities of such systems is of special interest for realization of SAD and TRADE Projects.

4. Neutron generator NG-12-1.

Neutron generator (Fig.12) [20] is linear accelerator of deuterium ions produced at duoplasmatron and accelerated to energy $\mathbf{E}_d$ = 250 keV. Accelerator magnet system separates

D^+ ions only that by means of electromagnetic lenses are directed towards the $Ti^3H_{1.5—1.8}$ or $TiD_{1.5—1.8}$ targets where in reactions $d(T,n)^4He$ and $d(D,n)^3He$ neutrons are generated with energies in the ranges E_n = 13-15 MeV and E_n = 2.5-3.0 MeV, respectively. At present highly effective water-cooled targets with diameters 230 and 45 mm are used in experimental program (Fig.13).

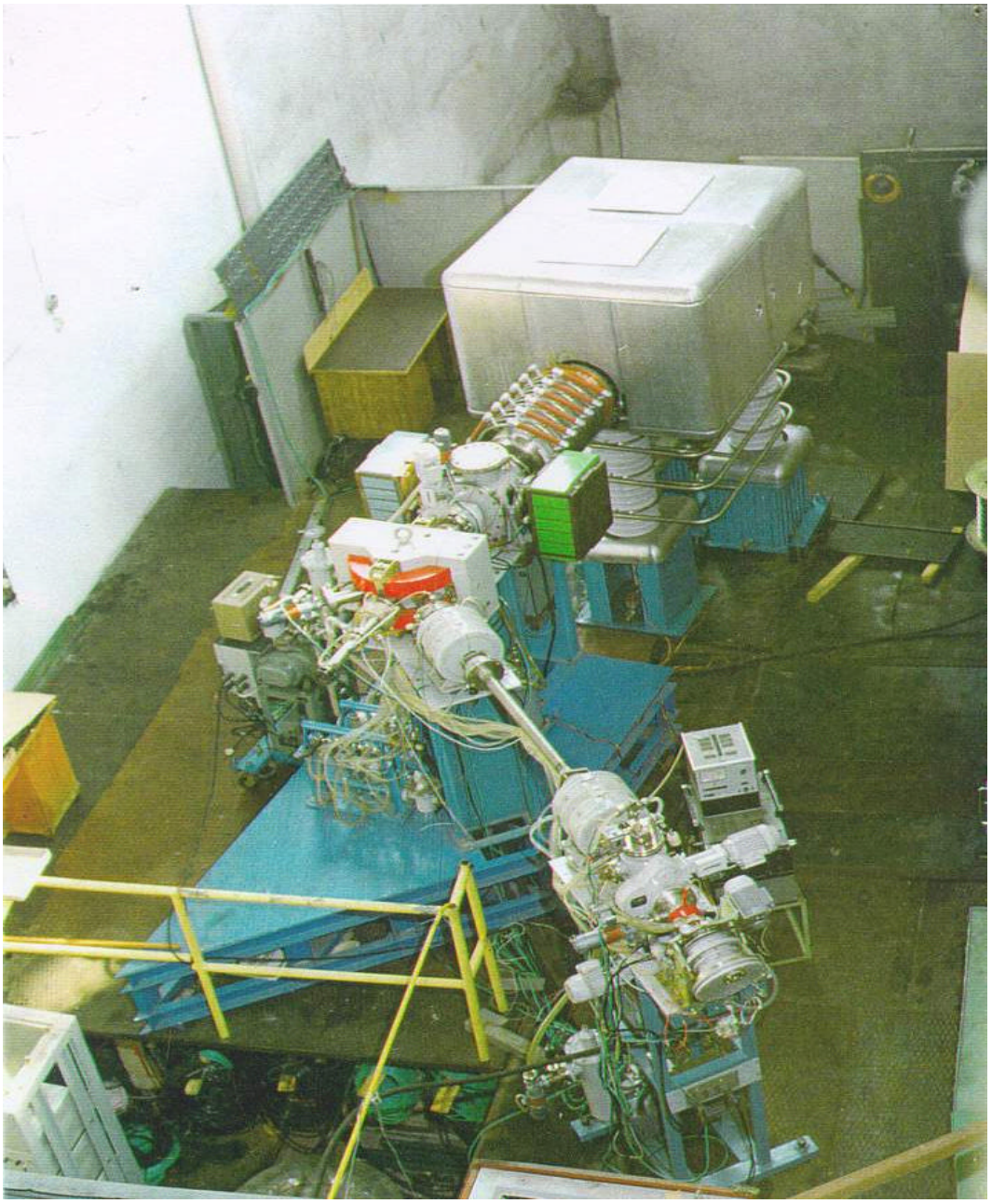

Fig. 12. General view of neutron generator NG-12-1.

By ion beam current Id ~ 12 mA yield of neutrons from targets with diameter 230 mm is about I ~ $1.5 \cdot 10^{12}$n/s for E_n = 13 - 15 MeV, I ~ (2.0 - 3.0) 10^{10}n/s for E_n = 2.5 - 3.0 MeV. For tritium and deuterium targets with diameter 45 mm neutron yields amount I ~ 1.5×10^{11}n/s and I ~ (2.0 - 3.0) $\times 10^{9}$n/s, respectively. By operation of neutron generator in pulse mode pulse duration can be set in the interval of 0.5 μs ≤ t ≤ 100 μs, pulse repetition frequency - 1Hz ≤ ω ≤ 10 kHz. For targets with diameter equal 45 mm special ion-guiding equipment was designed that allows to locate neutron source at each point of core including core center (Fig.13).

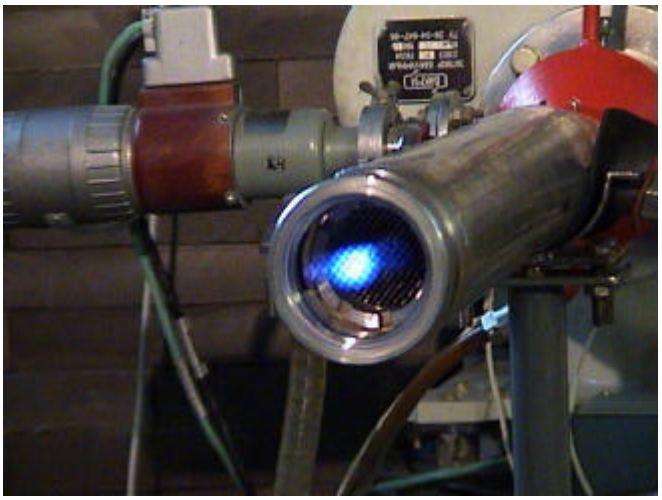

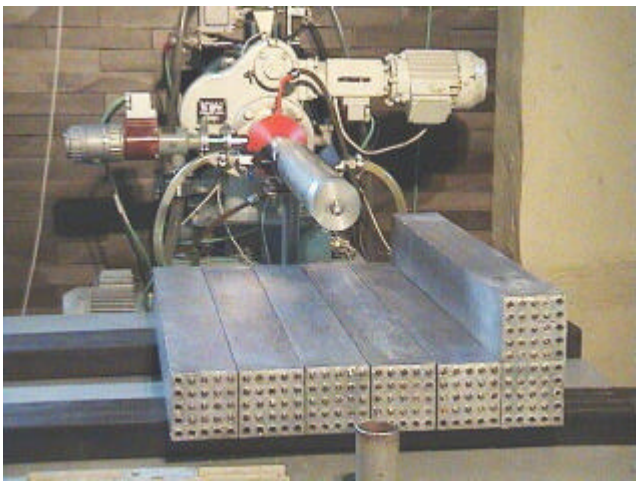

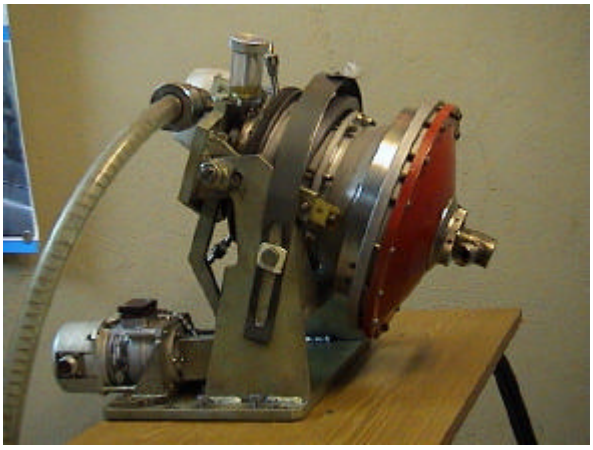

Target diameter
45 mm
Þ

Rotation speed	560 rpm
Target diameter	230 mm
Diameter of reaction space	100-200 mm
Tritium activity	0.53-0.75 MCi/kg
D/Ti (T/Ti) atomic ratio	1.5-1.8

Fig.13. General view of the neutron-producing targets with diameters 230mm, 45 mm and ion-guide system.

Main parameters of the neutron generator are presented in Table 1.

Table 1

Main parameters of the neutron generator NG-12-1

Accelerator	H+ and D+
Beam energy	100-250 keV
Beam current	1 - 12 mA
Pulse duration	$(0.5\text{-}100)\times10^{-6}$s
Pulse repetition frequency	(1-10 000) Hz
Spot size	2.0 -3.0 cm
Ti^3H target (230 mm):	
Rotation speed, rpm	560
Maximal yield of neutrons, n/s	$(1.5\text{-}2.0)\ 10^{12}$
Neutron energy	13-15 MeV
TiD target (230 mm):	
Maximal yield of neutrons, n/s	$(2.0\text{-}3.0)\ 10^{10}$
Neutron energy, MeV	2.5-3.0

The design of ion-guide device set and of neutron-producing targets was worked out so that source of external neutrons could be located at various points along Z-axis both inside and outside the core that allows to arrange various core configurations "external neutron source-core". The target with diameter 230 mm is located outside the core.

Monitoring of neutron yield from TiD and $Ti^{3H}H$ targets is being performed with application of foil activation analysis technique based on measurement of reactions ^{115}In (n,n^1) ^{115}In, ^{58}Ni (n,p) ^{58}Co rates for neutrons with energy E_n ~ 2.5 MeV (TiD-target) and of reactions ^{65}Cu (n,2n) ^{64}Cu and ^{58}Ni (n,p) ^{57}Co rates for neutrons with energy E_n > 13.0 MeV (Ti^3H-target).

5. Reactivity measurements

One of the important problems in physics of sub-critical systems driven by external neutron sources is development of experimental methods and techniques of neutron flux density monitoring and sub-criticality level determination without special procedure of criticality state achievement. Moreover it is important to verify the applicability of experimental methods used in physics of critical reactors for measurements of neutron-physical characteristics of systems both with thermal and fast neutron spectra.

The reactivity measurements at sub-critical systems driven by external neutron sources have been carried out with application of developed for critical systems methods such as:

5.1. Pulse neutron source method

Time evolution of neutron flux density (count rates of detector) in sub-critical system after the action of neutron pulse in assumption that neutron lifetime within one fission chain remains constant is expressed by the equation [21]:

$$\frac{dN}{dt} = B + Ae^{-at}$$

where $a = \frac{|r| + b_{eff}}{\Lambda}$ - fast neutron decay constant

$\Lambda = \frac{1}{k_{eff}} l$ (Λ - time of prompt neutrons generation, l – lifetime of prompt neutrons).

5.2. Sjöstrand method (area method)

This method is quite correct and is most often used for measurement of multiplication factor of sub-critical systems under the condition that external neutron source S(r,E) and subsequent fissions form in the core spatial flux distribution close to fundamental mode; energy distribution S(E) should approach to fission spectrum χ(E), energy and spatial distributions of fast $\Phi_{p,1}$ and delayed neutrons $\Phi_{d,1}$ should not differ significantly from solution of kinetic equation with lowest eigenvalue [22]. Elimination of highest harmonics i.e. deviation from fundamental solution of kinetic equation can be achieved by appropriate choice of external source position relative to the core center, detector position in the core, type of detector which sensitive layer material should be similar to fuel composition, or by application of 1/v detector by assumption that prompt and delayed neutrons have the same spectra. Close to optimum axial position of detector that allows to eliminate the influence of highest harmonics is within H′/3 < z < H′/3, where H′ is the extrapolated height of the core. The requirement of S(E) and χ(E) similarity in the case of sub-critical systems with neutron-producing target located at the core center is well satisfied because neutron spectrum in inelastic interactions of 14.1 MeV neutrons with lead nuclei and in (n,2n) reactions is formed mainly by slow (evaporation) stage of the reaction that results in neutron energy distribution almost identical to fission spectrum.

Formation of radial harmonics occurs due to neutrons of the external source that entering the reflector cause changes in distribution corresponding to fundamental mode, so for correct determination of the sub-criticality level is necessary to find appropriate radial position of detector and axial position of the external source by which the reactivity will not depend upon radius.

$$\frac{-r}{b_{eff}} = \frac{\text{prompt neutron area}}{\text{delayed neutron area}} \equiv \frac{I_p}{I_d}$$

5.3. Gozani method (modified method of Sjöstrand).

By application of Gozani method [23] the reactivity is expressed as:

$$-r(\$) = \frac{f \cdot A}{a \cdot B},$$

where r - reactivity in dollars;

A – amplitude of prompt neutrons flux;

f – frequency of pulse neutron source;

a – decay constant of prompt neutrons flux, s^{-1};

B – background of delayed neutrons.

5.4. Source jerk method.

Pulse mode of neutron generator operation allows to determine the level of sub-criticality by response of multiplying system to fast (fractions of microseconds) switching off the external neutron source. In the case when power of the sub-critical system with external neutron source is on the level N_1, defined by source intensity $S(\mathbf{r},E)$ and during the period equal to some intervals of prompt neutron lifetime after source switching off it passes to the level N_2 defined by delayed neutrons, the reactivity can be expressed by simple relation within point kinetics approach:

$$\frac{N_1 - N_2}{N_2} = \frac{r}{b_{eff}};$$

A modification of the method of sub-criticality measurement in the range of $\frac{r}{b_{eff}} < 5$, which accuracy near $\frac{r}{b_{eff}} \approx 2$ is about 3-4% (without taking into account the error in b_{eff} estimation) has been proposed in the work [24]. In the frame of this approach the reactivity in fractions of b_{eff} is defined by equation:

$$-\frac{r}{b_{eff}} = \left(\frac{N_1}{N_t} - 1\right) \cdot j(t)$$

where $j(t) = \sum_i \frac{b_i}{b} \cdot e^{-l_i t}$, N_1 - is detector counting rate in the presence of external neutron source after the equilibrium state is achieved, N_t detector counting rate at the moment *t (t < l).* Method does not take into account the influence of highest harmonics, it allows to make better the accuracy of N_t measurement after source removal, to determine the relation $-\frac{r}{b_{eff}}$ for each channel in time interval $l < t < 50ms, 100ms, ...1s$, to adjust the obtained reactivity magnitude to constant value or to take arithmetical mean of the obtained values.

In Table 2 input data for $j(t)$ calculation are presented (without correction for fast neutron fission).

Table 2.

Characteristics of groups of delayed neutrons by thermal neutron fission

	Groups of delayed neutrons					
	1	2	3	4	5	6
Decay constant l_i, s^{-1}	0.0124	0.0305	0.111	0.301	1.14	3.01
Relative fraction, b_i / b	0.033	0.219	0.196	0.395	0.115	0.042

The relation $N_t = \frac{N_1}{1 - \frac{r}{b_{eff}} / j(t)}$ allows to determine $\frac{r}{b_{eff}}$ by measurement of counting rate for wide time intervals before and after switching off the external neutron source by means of appropriate parameterization technique.

The result is fitted to analytical relation that includes characteristics of groups of delayed neutrons generated by thermal neutron fission of ^{235}U with variables: N_1-counting rate in the channel and ρ – sub-criticality of system in units of ß:

$$N_t = N_1/(1+r/(0{,}033 \cdot \mathrm{EXP}(-0{,}0124 \cdot X)+0{,}219 \cdot \mathrm{EXP}(-0{,}0305 \cdot X)+$$
$$+0{,}196 \cdot \mathrm{EXP}(-0{,}111 \cdot X)+0{,}395 \cdot \mathrm{EXP}(-0{,}301 \cdot X)+0{,}115 \cdot \mathrm{EXP}(-1{,}14 \cdot X)+$$
$$+0{,}042 \cdot \mathrm{EXP}(-3{,}01 \cdot X)))$$

By application of this method the restriction connected with device error at high level of neutron flux density is taken off that is important by measurement of deep sub-criticality, however in this case by calculation of $j(t)$ the correction of b_i is necessary taking into account neutron spectrum and fuel enrichment.

It should be noted too that combination of these methods of reactivity measurement allows to obtain kinetic parameters: β, Λ, ρ of sub-critical system driven by external neutron source (neutron generator).

By measurement of reactivity with application of the first three methods pulse duration of $d(T,n)^4He$ or $d(D,n)^3He$ neutrons was set to be equal t = 7μs, pulse repetition frequency

f = 54 Hz, channel width - 5 μs by total number of channels equal to 3600.

Time measurements have been carried out with application of fission chambers - CNT-5 (diameter – 7mm, detector length 70 mm, sensitive layer length – 5mm, sensitivity – 5×10^{-4} (pulse/s)/(n/cm^{2}s^{-1}), fissile nuclide – ^{235}U, filling gas – (98% A_2 + 2% N_2), m (^{235}U) = 1 mg; CNT-54 (diameter – 50mm, detector length 242 mm, sensitive layer length – 220 mm, sensitivity – 0.5 (pulse/s)/(n/(cm^{2}s^{-1}), fissile nuclide – ^{235}U, filling gas – (98% A_2 + 2% N_2), m (^{235}U) = 1 g, and small size (length - 1 cm and diameter – 1cm) ^3He neutron detector with sensitivity 0.5 (pulse/s)/(n/cm^{2}s^{-1}).

The electronic measuring equipment used for experiments at the YALINA facility consists of developed in the framework of ISTC – project fast-acting and low noise pre-amplifier compatible with fission chambers and of time analyzer TURBO MCS (ORTEC) having next parameters:

- maximum counting rate 150 MHz;
- channel width 5 ns – 65 535s;
- pass length to 16 384 channels
- memory capacity 16 777 215 counts/channel;
- input amplitude from -5B to +5B;
- minimum input pulse width 3 ns.

The results of k_{eff} measurements by application of various methods for core configuration with fuel rod number Nr = 280 (Fig.14) and for configurations when central and peripheral fuel rods are removed (Figures 15-18) are presented in Table 3.

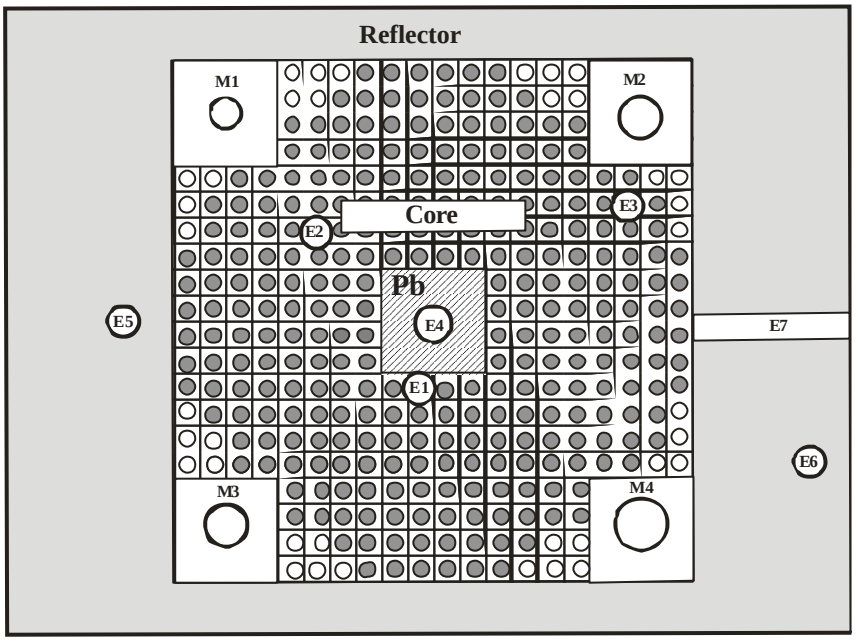

Uranium-polyethylene subcritical assembly

C - cross-section (280 fuel rods)
E1 - E7, M1 - M4 - experimental channels

Fig. 14. Core configuration of the sub-critical assembly with fuel rods number N_r=280.

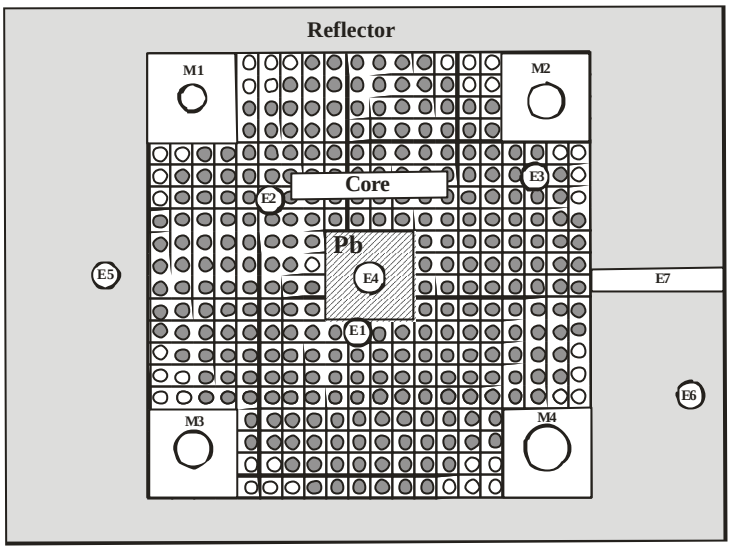

Uranium-polyethylene subcritical assembly

C - cross-section (279 fuel rods)
E1 -E 7, M1 - M 4 - experimental channels

Fig.15. Core configuration of the sub-critical assembly with fuel rods number N_r=279 (one fuel rod is removed from central part of core)

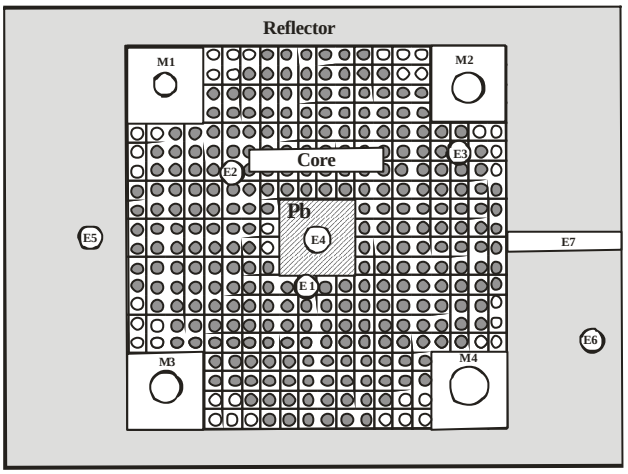

Uranium-polyethylene subcritical assembly

C - cross-section (278 fuel rods)
E1 - E 7, M1 - M4 - experimental channels

Fig. 16. Core configuration of the sub-critical assembly (with fuel rods number N_r=278). (two fuel rods are removed from central part of the core).

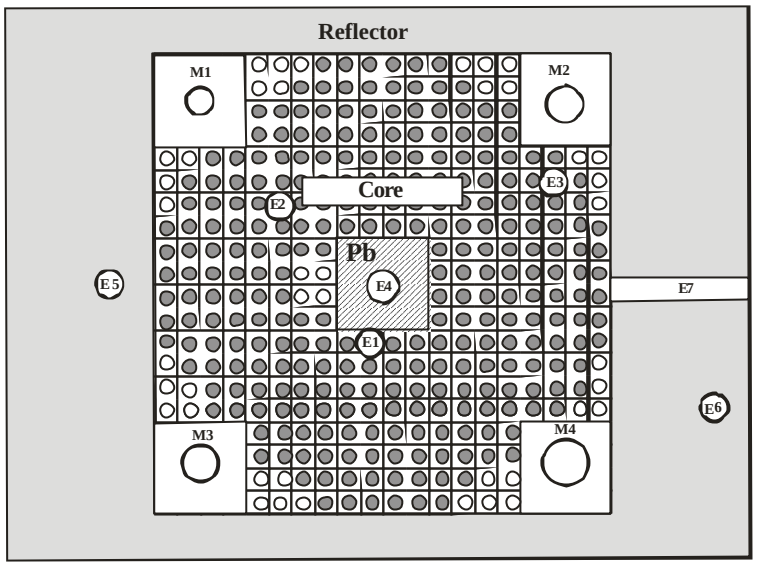

Uranium-polyethylene subcritical assembly

C - cross-section (276 fuel rods)
E1 -E 7, M1 - M4 - experimental channels

Fig. 17. Core configuration of the sub-critical assembly with fuel rods number N_r=276 (four fuel rods are removed from central part of the core).

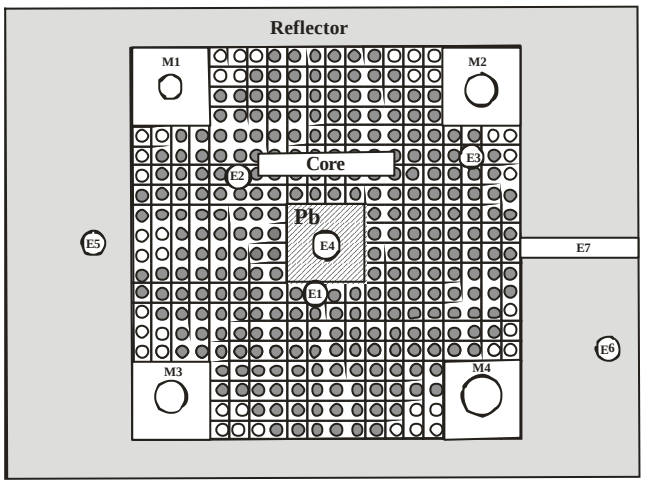

Uranium-polyethylene subcritical assembly

C - cross-section (276 fuel rods)
E1 -E 7, M1 - M4 - experimental channels

Fig. 18. Core configuration of the sub-critical assembly with fuel rods number N_r=276 (four fuel rods are removed from peripheral part of the core).

In the table 3 the values of k_{eff} and of neutron lifetime calculated with application of MCNP-4B code [25] are there presented too. The value of β_{eff} was estimated by code

KRATER intended for calculation of critical systems with thermal neutron spectrum [26]. Effective part of delayed neutrons was calculated by equation:

$$b_{eff} = \frac{\int_V dV \sum_l \sum_j \left(n_f \Sigma_f\right)_{l,j} b_l \Phi_j \Phi_5^*}{\int_V dV \sum_k \left[\sum_j \left(n_f \Sigma_f\right)_j\right] c_k \Phi_k^*}$$

where Φ_j-neutron flux in energy group j, Φ_j^*-neutron importance in energy group j, b_l – part of delayed neutrons of group i of predecessor of delayed neutrons by fission of nuclide l, l-index of fissile nuclide, c_k prompt neutron spectrum, V - core volume. Just the obtained value - β_{eff} = $7.37 \cdot 10^{-3}$ was taken into account by calculation of sub-criticality level with application of above - mentioned methods. As it follows from presented data experimentally measured reactivity values are close enough to those calculated by MCNP-4B code.

Table 3.

Experimental and calculated reactivity of sub-critical assembly of various configurations

N_{rods}	Pulse Neutron Source Method			Gozani Method		Keff (1/N)	Sjöstrand Method		Keff MCNP	Life time, μs (MCNP)
	a, s-1	ρa, $	Keff_a	ρGozani, $	k_{eff}_Gozani		ρS, $	k_{eff}_S		
280 rods	451,6 ±1,4	4,154	0,969	4,397	0,967	0.964	4,547	0,967	0.9715 ± 0.0007	94.1
280 - 1 central rods	473,1±1,7	4,399	0,968	4,844	0,964	0.962	5,205	0,962	0.9686 ± 0.0007	94.4
280 - 2 central rods	486,1±1,6	4,548	0,966	4,832	0,964	0.960	5,219	0,962	0.9665 ± 0.0007	94.9
280 - 4 central rods	519,6±2,0	4,930	0,964	5,365	0,960	0.955	5,898	0,957	0.9616 ± 0.0006	95.99
280 – 1 peripheral rods	458,6±1,05	4,240	0,969	4,307	0,968	0.963	4,536	0,967	0.9703 ± 0.0007	94.04
280 – 2 peripheral rods	468,4±1,1	4,346	0,968	4,442	0,967	0.962	4,595	0,966	0.9689 ± 0.0007	94.3
280 – 4 peripheral rods	490,5±1,23	4,598	0,966	4,679	0,965	0.960	5,052	0,963	0.9672 ± 0.0007	94.4

In Figures 19, 20 time dependence of measured counting rates for three core configurations with fuel rod numbers Nr =276, 278, 279 and 280 is presented that demonstrates the influence of central and peripheral fuel rods on time evolution of neutron flux density in the core after the action of pulse of neutrons generated in reaction d (T,n) ^{4}He.

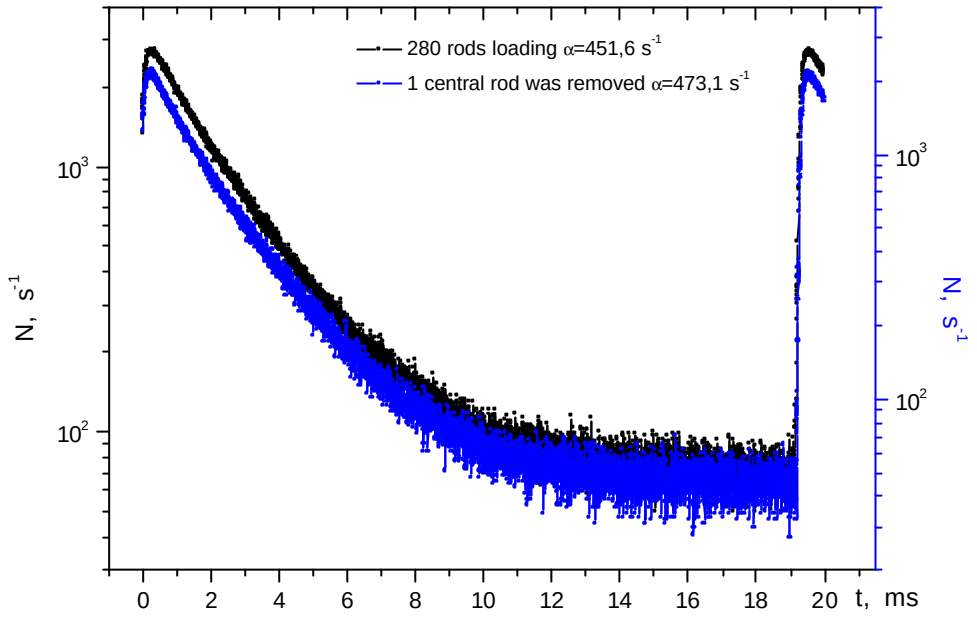

Fig. 19. Time distribution of neutron flux density in the sub-critical assembly by core configurations with 280 and 279 fuel rods. Measurements were made at center of the experimental channel E 2 by fission chamber with ^{235}U - CNT-5

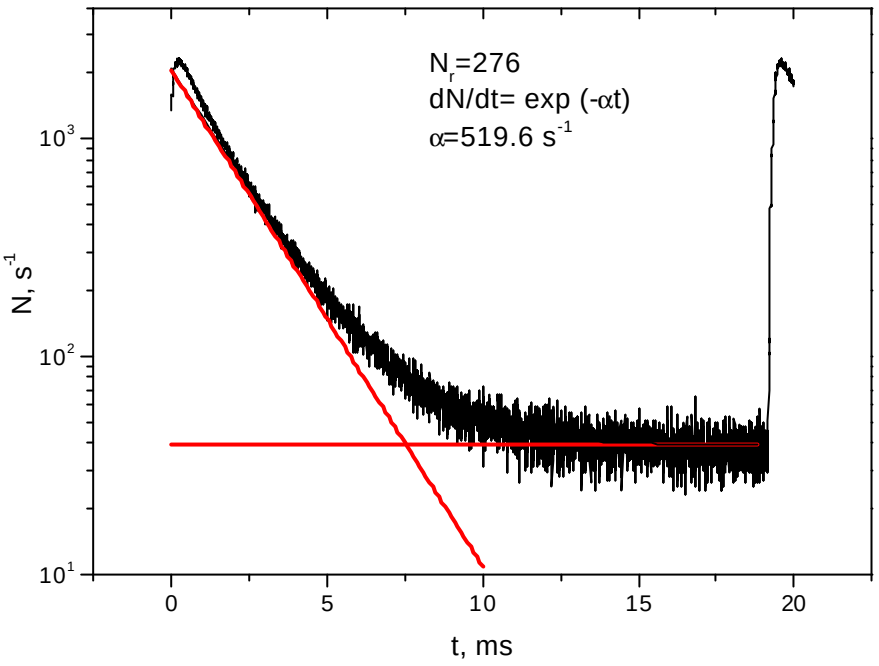

Fig. 20. Time distribution of neutron flux density in the sub-critical assembly for core configuration with 276 fuel rods. Measurements were made at center of the experimental channel E 2.with application of fission chamber with ^{235}U - CNT-5.

Neutron flux time evolution caused by impact of pulse neutron source located outside the core at the distance of -54.5 cm from the core center has been measured with application of ^{235}U fission chambers and ^{3}He – detector at central part of the core experimental channels. It is presented in Figure 21. One can see that neutron flux variation rate is the same in all experimental channels i.e. it does not depend upon radius.

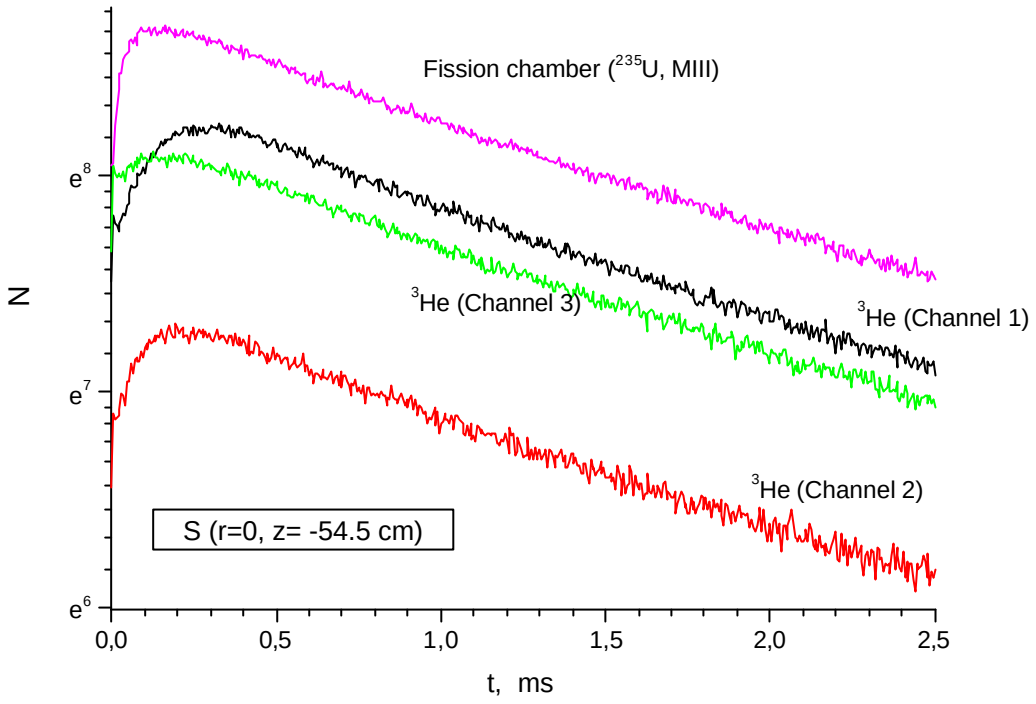

Fig. 21. Time behavior of neutron flux density measured with application of ^{235}U fission chamber - CNT-5 and ^{3}He-detector in the experimental channels of the core loaded by N_r = 280.

Reactivity measurements at sub-critical assembly with fuel rod number N_r = 280 have been performed with application of Feynman-α method too.

$$\frac{\overline{C}^2 - \overline{C}^2}{\overline{C}} = 1 + \frac{\varepsilon D_g}{r_p^2}\left(1 - \frac{e^{-a t}}{a t}\right)e^{-a t} = 1 + Y$$

where C - counts number being registered during τ - time interval, α constant of neutron flux decay; ε - detection efficiency; D_γ - Diven factor (for ^{235}U D_γ = 0.796);

$$r_p = \frac{k-1}{k};$$

$$a_{Feynman} = \frac{1-k_p}{l},$$

where *N*- neutron number at the assembly, k_p – multiplication factor on prompt neutrons, l – prompt neutrons lifetime.

Measurements were performed with application of ^{252}Cf spontaneous fission neutron source with intensity I=3.75·10^5 n/s located at the core center and ^{3}He detector (ε = 3.14·10^{-4} pulse/fission). Time interval for the measurements was chosen to be equal T ≤ 100 ms. The

value of α = 538 ±43 obtained by fittng of Y is close enough to α obtained by pulse neutron source method (Fig. 22).

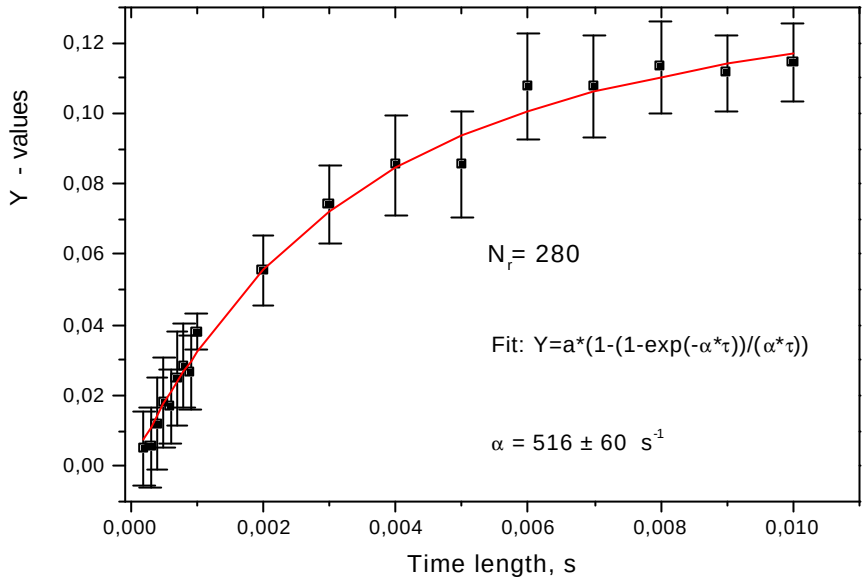

Fig.22. Feynman Y(t) values for ^{252}Cf source.

With the purpose of investigation of neutron-producing Pb, (Pb-Bi) targets influence on core parameters, study the target and core coupling effects at center of the YALINA core a lead zone was inserted where either external neutron sources with neutron energies 14.1 MeV and 2.5 MeV or source of neutrons from ^{252}Cf spontaneous fission could be located. X-Z cut of the sub-critical assembly YALINA-Pb core configuration with fuel rod number N_r = 280 is presented in Fig. 23. X-Y cut of the sub-critical assembly YALINA-Pb core configuration with fuel rod number N_r = 280 is presented in Fig. 24. As an example of reactivity estimation by source jerk method counting rates of ^{3}He-detector measured in the experimental channel EC-3 before and after switching off neutron generator are shown in Fig. 25.

In this measurement the Ti^{3}H target of neutron generator with diameter equal to 45 mm was located at center of the lead zone of sub-critical assembly (Fig. 24)

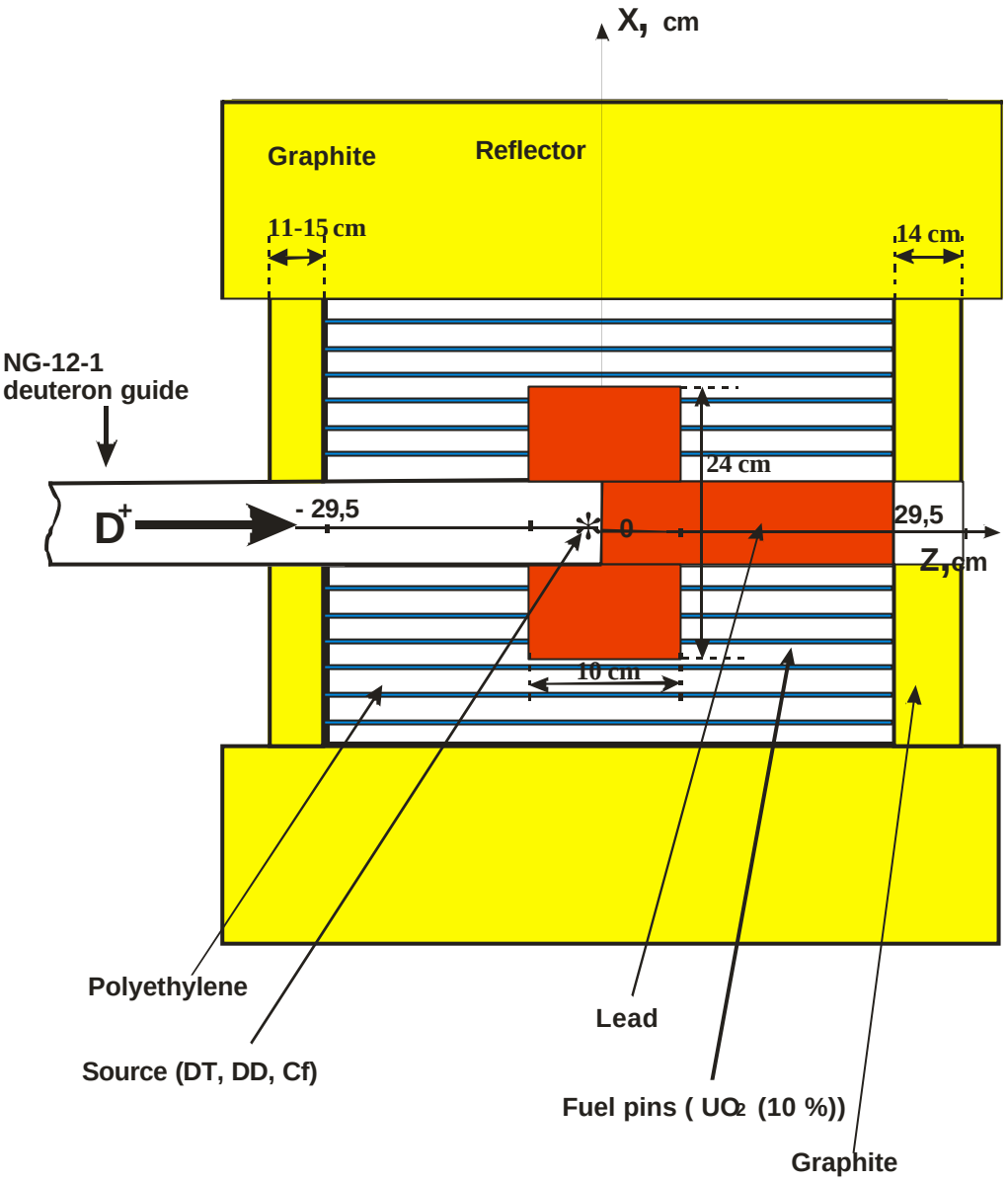

Longitudinal section of source-core configuration for 280 fuel pins

Fig. 23. X-Z cut of the YALINA-Pb sub-critical configuration with lead zone in the core center.

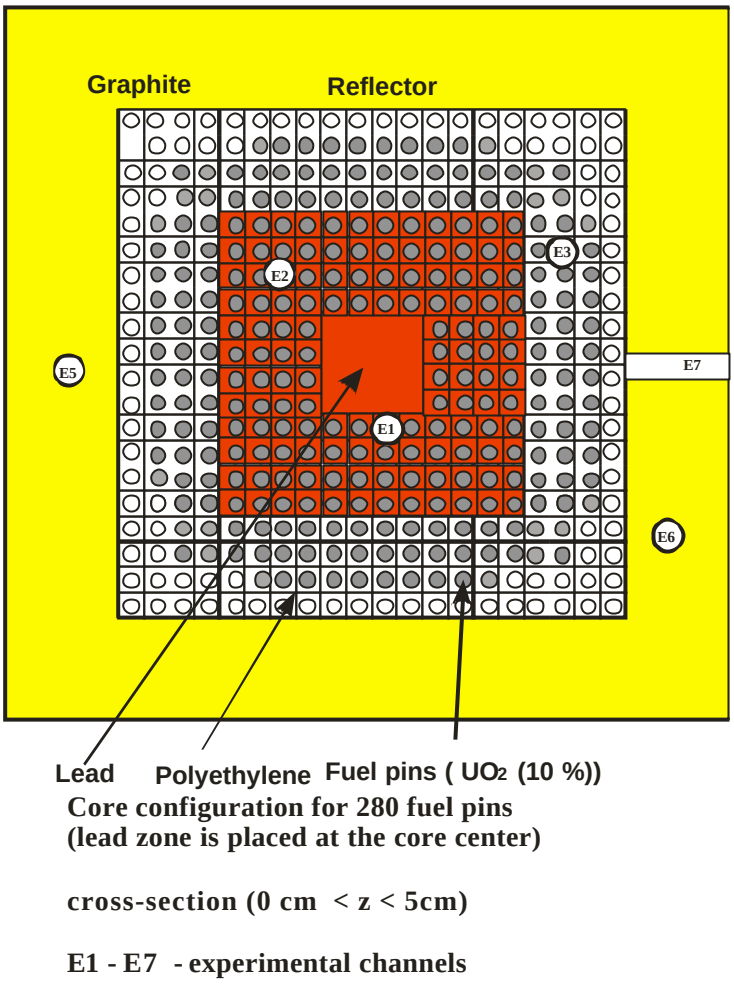

Fig.24. X-Y cut of the core configuration with lead zone.

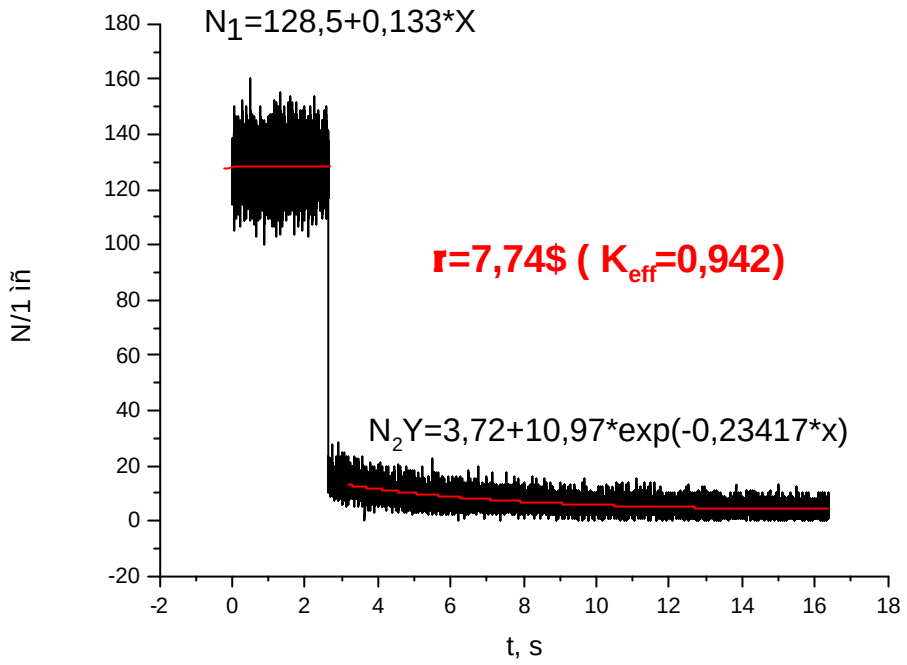

Fig.25. Time dependence of ^{3}He-detector counting rate by reactivity estimation of the sub-critical system with lead zone (YALINA-Pb) by source jerk method (^{3}He was located at center of the experimental channel EC 3).

Time distribution of neutron flux density in assembly with lead zone at the core center have been measured in the reflector (channel EC 6) and in experimental channel EC 3 after the pulse of neutrons with energy 14.1 MeV, duration 7 μs. The results of the measurements are presented in Fig. 26.

It is seen that presence of the lead zone at the core center is the reason of remarkable variation of dN/dt distribution in the reflector due to moderation of neutrons formed in lead zone in U(n,f) and Pb(n,2n), U (n,2n) reactions in high energy range.

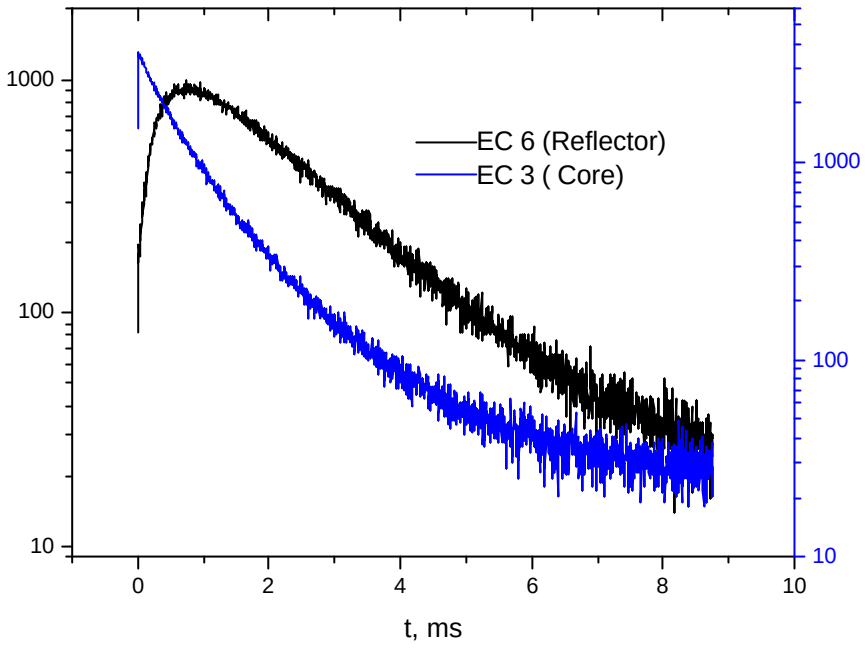

Fig. 26. Time dependence of ^{3}He – detector counting rates in the experimental channels EC 3 (core) and EC 6 (reflector) of the sub-critical assembly YALINA-Pb.

As can be inferred from the presented information, the measurements of sub-critical system reactivity based on pulse neutron source method should be performed inside the core because contribution of source neutrons to neutron flux time behavior in reflector can be high enough to result in distribution different from $dN/dt \sim e^{-a\,t}$ that follows from point kinetics approximation.

6. Energy and spatial distributions of neutrons in the core of the sub-critical assembly.

Energy distribution of neutrons in the sub-critical systems is main parameter that defines most of ADS-technology characteristics and first of all transmutation of minor-actinides and long-lived fission fragments. Experimental measurement of neutron spectrum in such systems is non-trivial because of a great number of reactions in high energy range (n, xn,yp) that to a great extent influence the shape of neutron energy distribution in the core.

Unfolding of neutron energy spectra was performed on the basis of method of threshold (n,xn,yp) reactions effective cross-sections that was developed for determination of neutron spectrum in experiments at deeply sub-critical system with lead neutron-producing target, surrounded by uranium fuel rods with natural uranium (0.7 % of ^{235}U), irradiated by proton beam with proton energy E_p = 1.5 Gev [27]. The method is reduced to solution of Fredholm integral equations set of first kind and does not demand knowledge of the reference spectrum. For determination of neutron energy spectrum at YALINA facility the following reactions were used:
^{111}Cd (n,n') $^{111}Cd^m$ (E_{eff} = 0,25 MeV),$^{55}Mn(n,a)^{52}V$ (E_{eff} = 0,64 MeV), $^{204}Pb(n,n')^{204}Pb^m$ (E_{eff}=0,90 MeV), $^{115}In(n,n')^{115}In^m$ (E_{eff}=0,34 MeV), $^{90}Zr(n,p)^{64}Cu$ (E_{eff}=2,0 MeV), $^{58}Ni(n,p)^{58}Co$ (E_{eff}=2,7 MeV), $^{59}Co(n,p)^{59}Fe$ (E_{eff}=2,8 MeV), $^{65}Cu(n,p)^{65}Ni$ (E_{eff}=3,5 MeV), $^{27}Al(n,p)^{27}Mg$ (E_{eff} = 4,5 MeV), ^{24}Mg $(n,p)^{24}Na$ (E_{eff}=4,93 MeV), ^{48}Ti $(n,p)^{48}Sc$ (E_{eff}=5.0 MeV), $^{56}Fe(n,p)^{56}Mn$ (E_{eff} = 6,60 MeV), $^{59}Co(n,a)^{56}Mn$ (E_{eff}=7,10 MeV), $^{27}Al(n, a)^{24}Na$ (E_{eff} = 7,45 MeV). Analysis of gamma-quantum spectra was performed with application of germanium detector with efficiency 80%, energy resolution - 1.1 keV for E_γ =122 keV and 2.1 keV for E_γ =1332 keV. Detector was placed in combined shielding of cylindrical shape made of low background steel components, lead, copper and cadmium with total weight about 1 ton.

Neutron spectrum in energy range 0.3-13.0 MeV measured at the core center with application of developed method is compared in Fig. 27 with spectrum calculated by MCNP-4B code. It is evident that results of calculations agree well enough with experimental data. It should be noted that developed method is of special interest from the point of view of neutron and proton spectra measurement at SAD facility (sub-critical assembly with MOX fuel driven by proton accelerator with E_p = 660 MeV) in energy range from a few keV up to E~100

MeV, that is of special interest for verification of codes of nucleon-meson cascade calculation because in this energy range the contribution of pre-equilibrium emission is predominant.

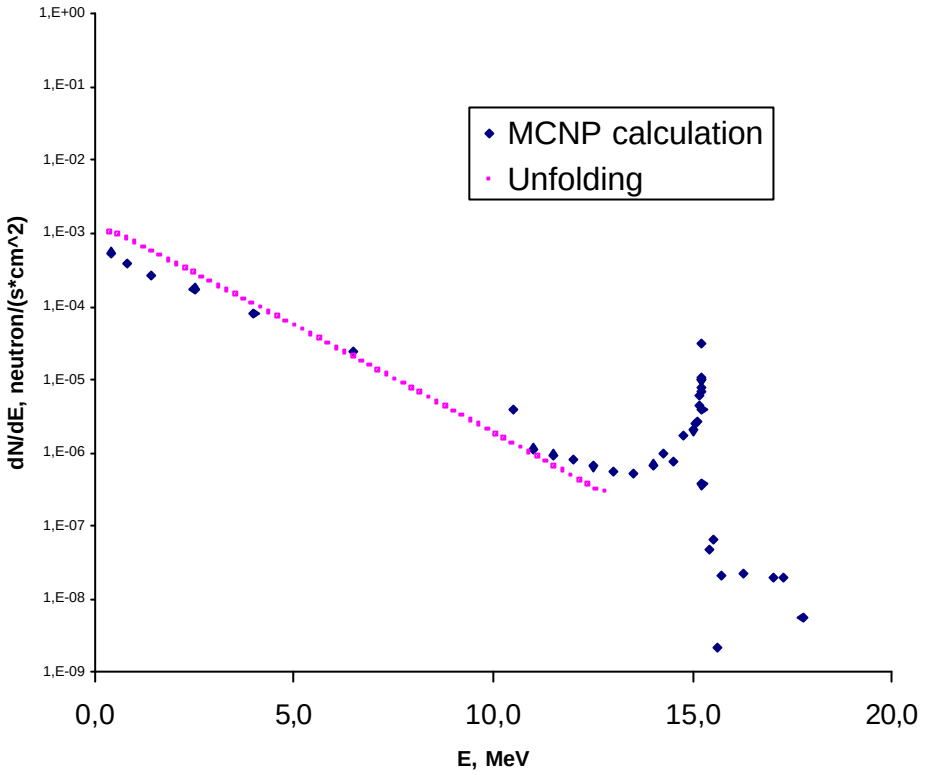

Fig.27. Comparison of neutron spectra in sub-critical assembly YALINA at the point Z=0 cm and R=11 cm calculated by MCNP-4B code and unfolded by method of effective cross sections of threshold reactions using experimental data in the energy range 0.4 - 13 MeV, per one neutron generated by NG-12-1 operating in (d,t) mode.

One of the main characteristics of thermal neutron spectrum is cadmium ratio R_{Cd} that demonstrates the contribution of thermal neutrons to the total neutron spectrum. Comparison of calculated and experimental data on radial distribution of cadmium ratio for reactions $^{237}Np(n,\gamma)^{238}Np$ and $^{243}Am(n,\gamma)^{244}Am$ in the core driven by external neutron source $d(T,n)^4He$ located outside the core (Z = - 38.0 cm) is demonstrated in Fig. 28. Radionuclides ^{237}Np and ^{243}Am in the form of NpO_2 and AmO_2 samples (Table 4) were placed into cadmium containers with wall thickness d = 1.5 mm and then located at central part of the core experimental channels (E1, E2, E3).

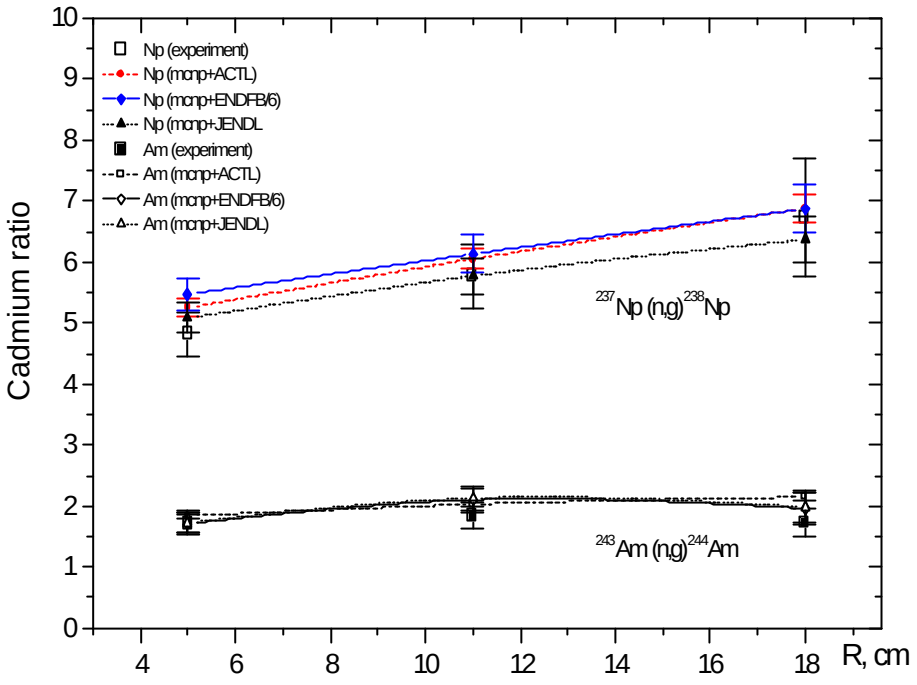

Fig. 28. Experimentally measured and calculated cadmium ratios for ^{243}Am (n, γ) and ^{237}Np (n, γ) reactions by using ACTL, ENDFB/6 and JENDL libraries of evaluated nuclear data.

Table 4

Characteristics of radioactive targets.

Sample	Activity, 10^8 Bq	Mass, mg	Admixture
NaI	0.044	1	< 17% ^{127}I
NpO_2	0.113	366	< 0.2% ^{239}Pu
Am O_2	1.100	14.8	< 0.2% ^{239}Pu

One can see that cadmium ratio increases by about 30% to the core periphery, that is the evidence of increasing of contribution of neutrons with energy less than $E < E_{Cd} = 0.5$ eV to energy distribution of neutron flux density. It should be noted too that such a behavior of R_{Cd} in the case of ^{237}Np is caused by peculiarities of energy dependence of cross section of ^{237}Np (n,γ) reaction which main resonances are below E_{Cd}. It can be drawn from the presented data that R_{Cd} for Am remains almost unchanged in direction from the core center to its periphery. The attention should be paid too that use of nuclear data taken from various libraries gives fairly close values of R_{Cd}. Measurements of neutron capture reaction rate of

^{237}Np nucleus performed in the presence of cadmium container and without it allow to estimate the contribution of neutrons with energies higher than E_{Cd} to transmutation reaction.

The results of measurements of spatial distribution of threshold reactions In (n,n`), ^{19}F(n,2n)^{18}F, ^{27}Al(n, a)^{24}Na rates in sub-critical core for sub-criticality level k_{eff} = 0.98 with external d (T,n)^{4}He neutrons source located outside the core are presented in Figures 29-35.

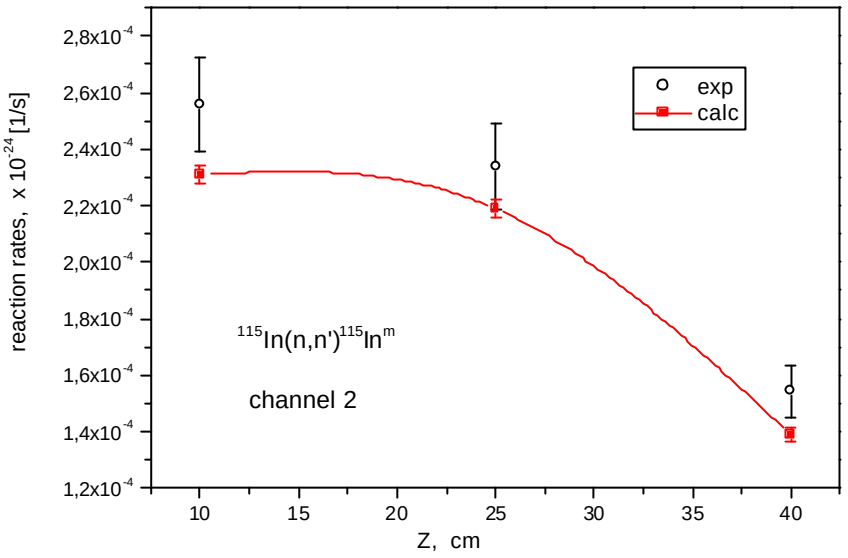

Fig. 29. Axial distribution of ^{115}I(n,n')^{115}In^{m} reaction rates in 2nd channel of the sub-critical assembly (normalized per one neutron from (d,d) reaction)

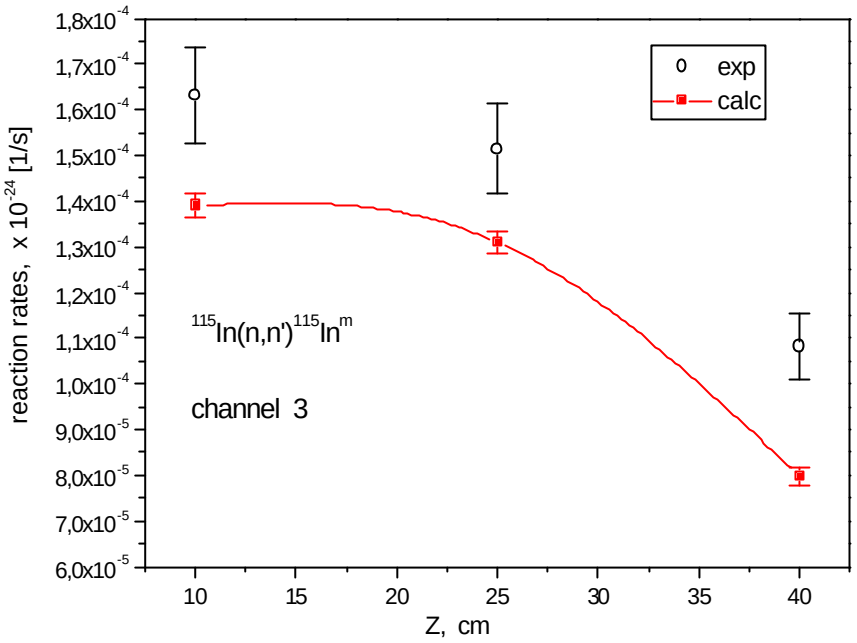

Fig. 30. Axial distribution of $^{115}I(n,n')^{115}In^{m}$ reaction rates in channel E3 of the sub-critical assembly (normalized per one neutron from (d,d) reaction)

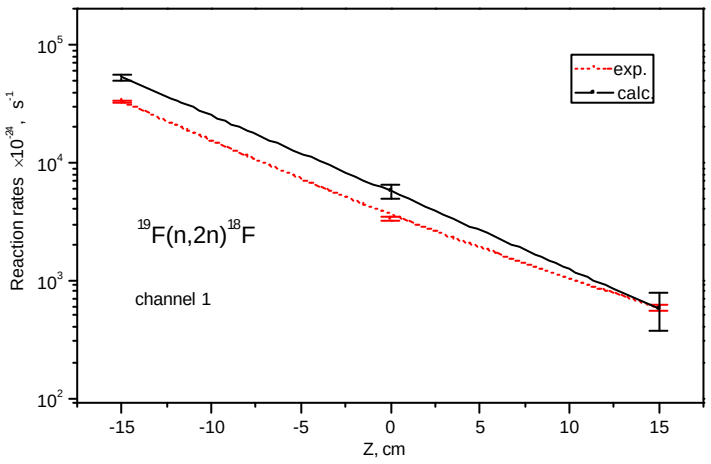

Fig. 31. Axial distribution of $^{19}F(n,2n)^{18}F$ reaction rate in channel E1of the core (R = 5 cm).

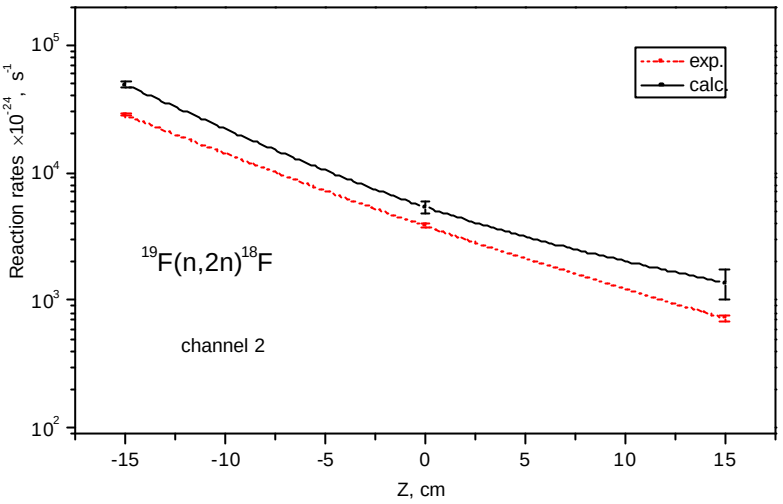

Fig. 32. Axial distribution of $^{19}F(n,2n)^{18}F$ reaction rate in channel E2 of the core (R = 11 cm).

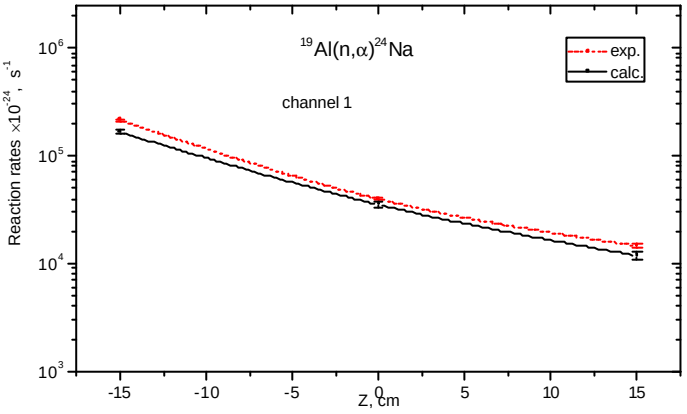

Fig. 33. Axial distribution of $^{27}Al(n,\alpha)^{23}Na$ reaction rate in channel E1of the core (R = 5 cm).

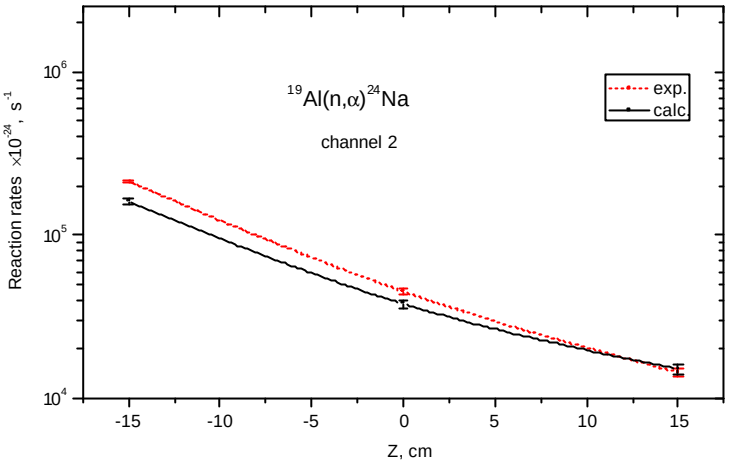

Fig. 34. Axial distribution of ^{27}Al(n, α)^{24}Na reaction rate in channel 2 of the core (R =11 cm).

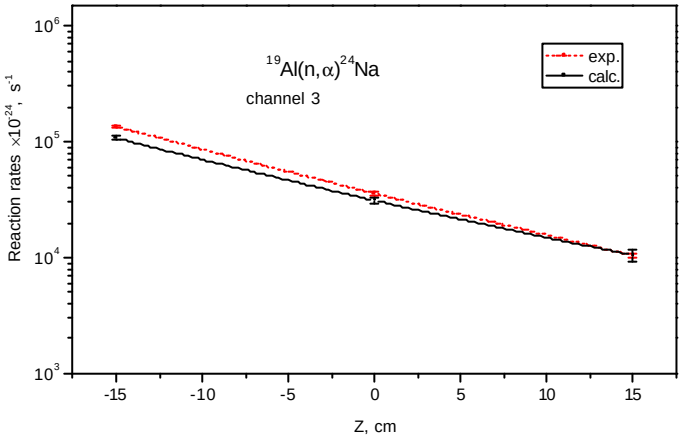

Fig. 35. Axial distribution of ^{27}Al(n, α)^{24}Na reaction rate in channel 3 of the core (R =20 cm).

Reaction rates calculated with application of MCNP-4B code and different libraries of evaluated nuclear data agree well enough with experimentally measured ones for majority of nuclear reactions (see for example ^{115}In (n,n") ^{115}In), however for several reactions such as ^{48}Ti(n,p)^{48}Sc,^{27}Al(n,p)^{27}Mg the discrepancy is observed.

As follows from presented results of experimental measurements the rates of threshold reactions decrease to the core periphery decreasing to be more significant than that of radiation capture reaction rates. Such behavior is a consequence of reducing of high energy neutron number due to both elastic and inelastic interactions with medium nuclei.

For each of the core configurations axial and radial neutron flux density distributions were measured by various external neutron sources and its' locations relative to the core

center. For illustration calculated radial distributions of neutron flux density by various neutron energies E_n < 1 eV, E_n > 100 keV, E_n > 0.75 MeV , E_n > 1.0 MeV as well as experimentally measured ones by means of ^{3}He detector for neutron source from ^{252}Cf spontaneous fission spectrum located at the core center and neutron source from reaction d(T,n) ^{3}He located outside the core at the distance Z = - 38 cm from core center are presented in Figures 36-38. One can see that calculated distribution of neutrons with energy E_n < 1 eV agree well with experimental data measured in the core and reflector both for ^{252}Cf neutron source and for 14.1 MeV neutron source located outside the core at the distance Z = - 38 cm from the core center. The attention should be paid to the fact that radial neutron flux distribution in sub-critical system with k_{eff}=0.98 differs significantly from distribution characteristic for critical systems which distribution is similar to $\Phi(r) \sim \cos(r)$.

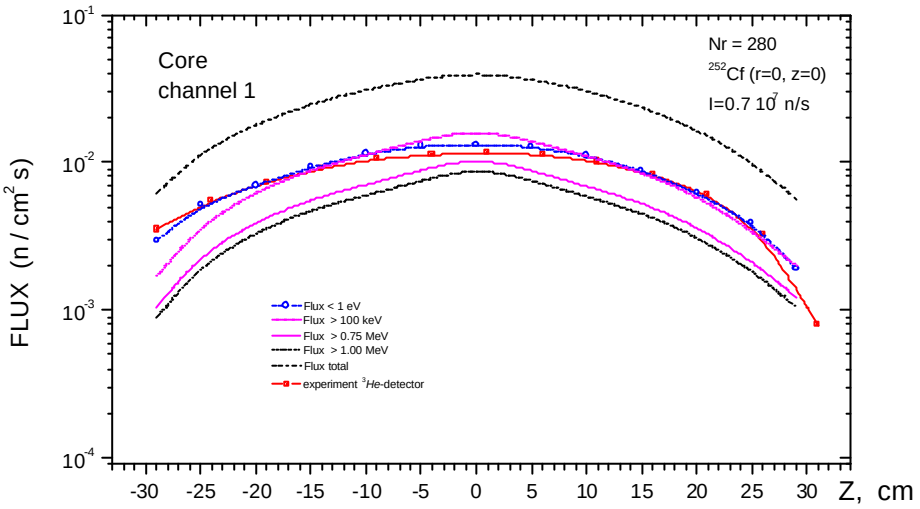

Fig. 36. Axial distribution of fast, thermal and total neutron flux densities in the experimental channel E1 (R=5 cm)

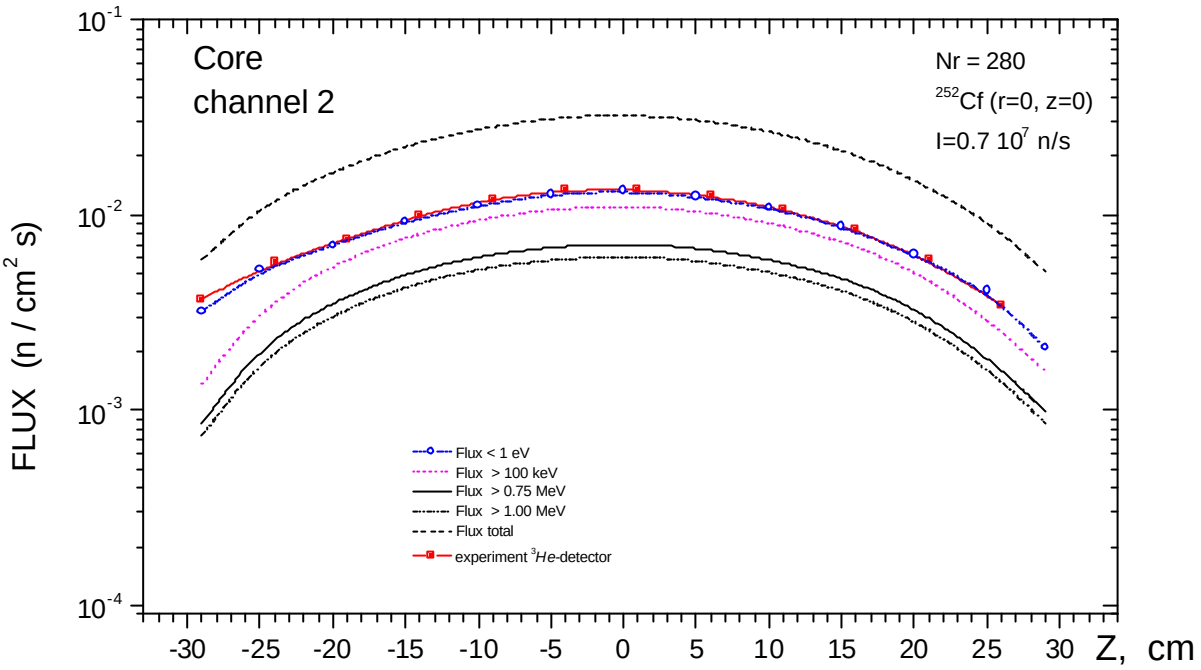

Fig. 37. Axial distribution of fast, thermal and total neutron flux densities in the experimental channel E2.

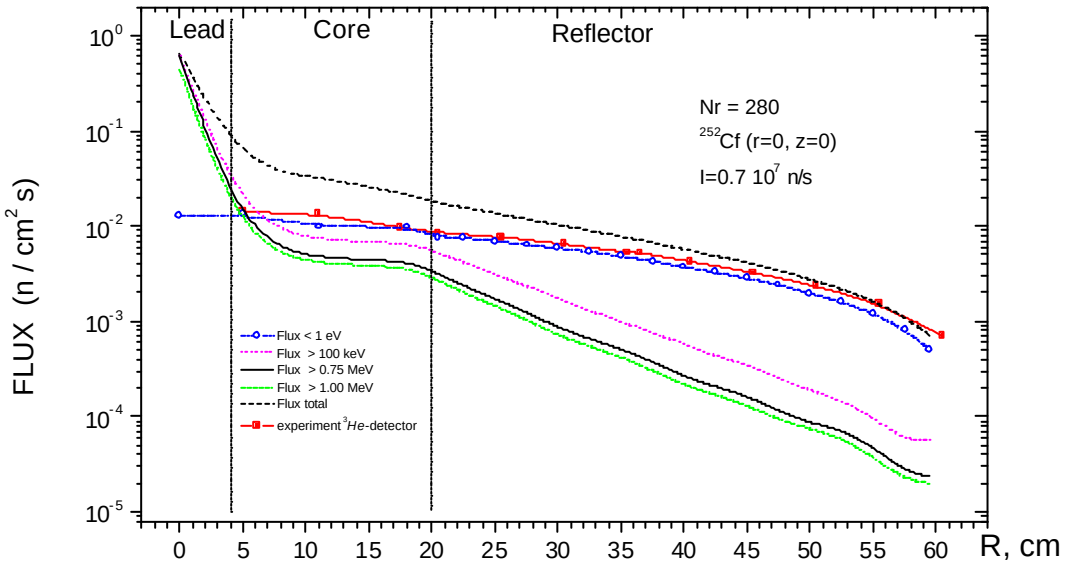

Fig. 38. Radial distribution of fast (E_n > 0.75 MeV), (E_n > 0.1 MeV) and thermal (E_n < 1 eV) neutrons flux densities and total neutron flux density in the sub-critical assembly. (^{252}Cf neutron source is located at the core center).

One of the main aspects of ADS-technology is transmutation of MA and LLFP of nuclear fuel cycle. In this connection YALINA facility due to high neutron flux density in the core, possibility of core sub-criticality level variation ($0.90 \leq k_{eff} \leq 0.98$), application of various neutron sources and configurations "external neutron source – core" gives a unique opportunity for investigation of the peculiarities of MA and LLFP transmutation in ADS with thermal neutron spectrum that is of special interest for testing computer codes and evaluated nuclear data libraries. For illustration in Figures 39-38 calculated and experimentally measured spatial distributions of $^{129}I(n,\gamma)^{130}I$, $^{237}Np(n,\gamma)\ ^{238}Np$ and $^{243}Am(n,\gamma)^{244}Am$ reaction rates in the core loaded by fuel rod number $N_r = 280$ in the case when sub-critical assembly is driven by neutron generator operating with deuterium target located outside the core at the distance 38 cm from it's center are presented. Gamma - spectra of radioactive nuclei ^{129}I, ^{237}Np, ^{243}Am (Table 4) and its' daughter nuclei are presented in Figures. 39-46. Fission products and minor actinides were irradiated in the core of the sub-critical assembly during 3 hours.

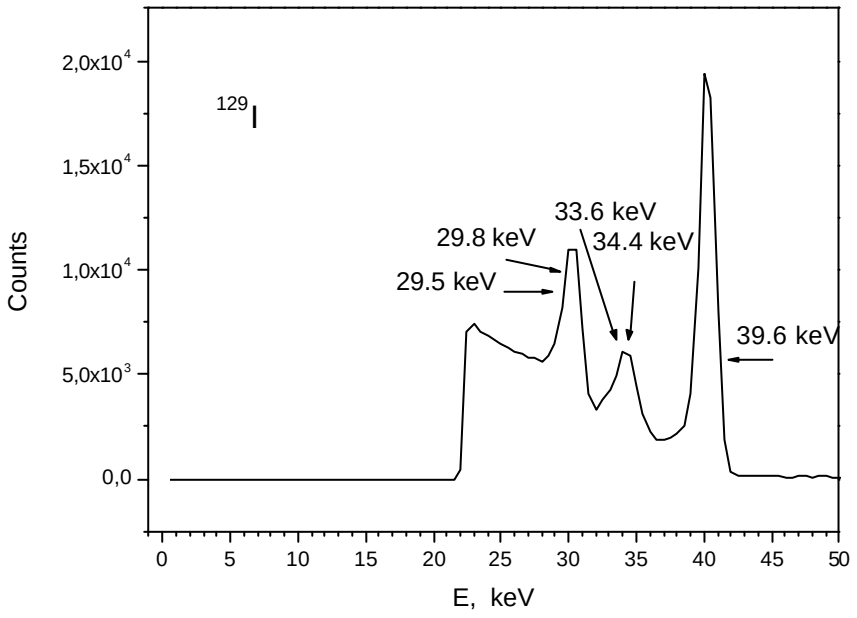

Fig. 39. Gamma - spectrum of ^{129}I.

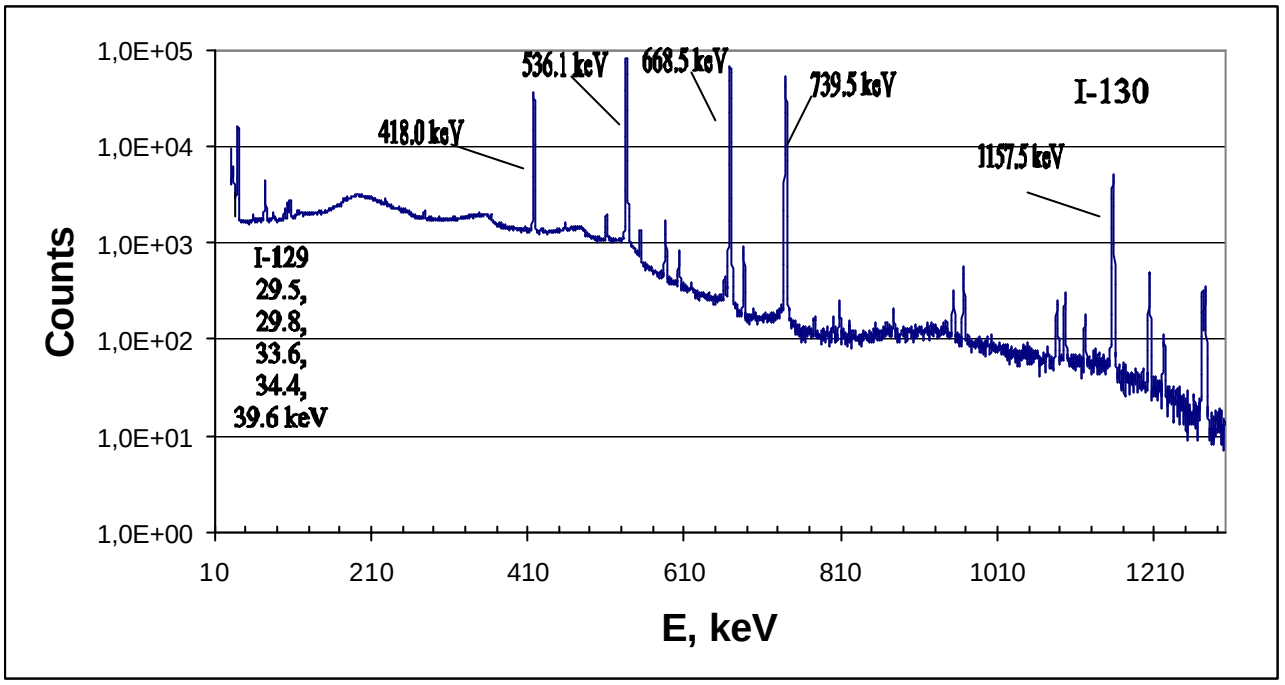

Fig. 40. Gamma - spectrum of ^{130}I.

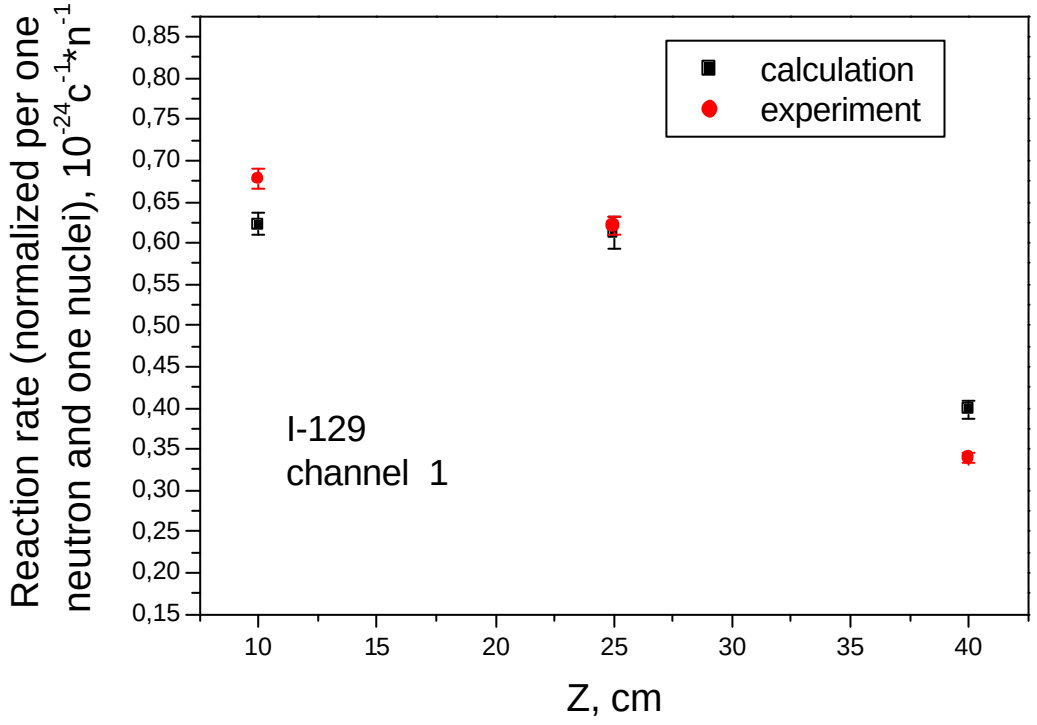

Fig. 41. Axial distribution of ^{129}I(n,γ)^{130}I reaction rate in the channel E1.

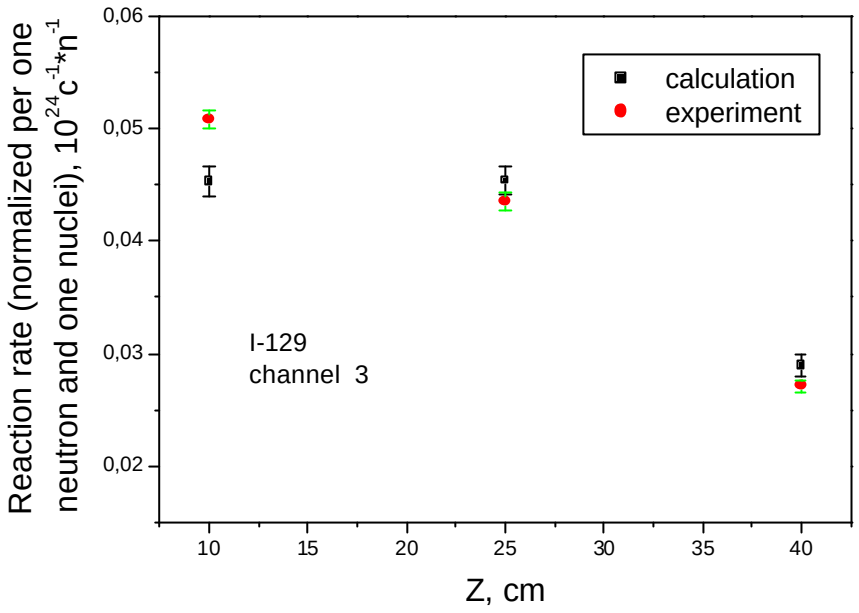

Fig. 42. Axial distribution of $^{129}I(n,\gamma)^{130}I$ reaction rates in the experimental channel E2. (R = 10 cm).

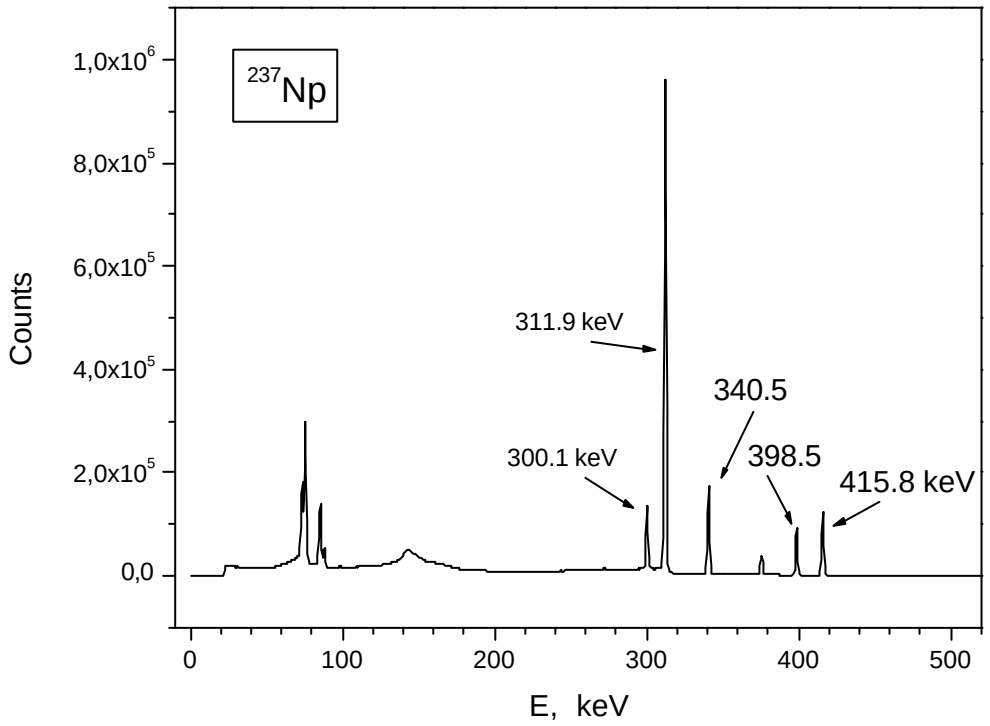

Fig. 43. Gamma-spectrum of ^{237}Np.

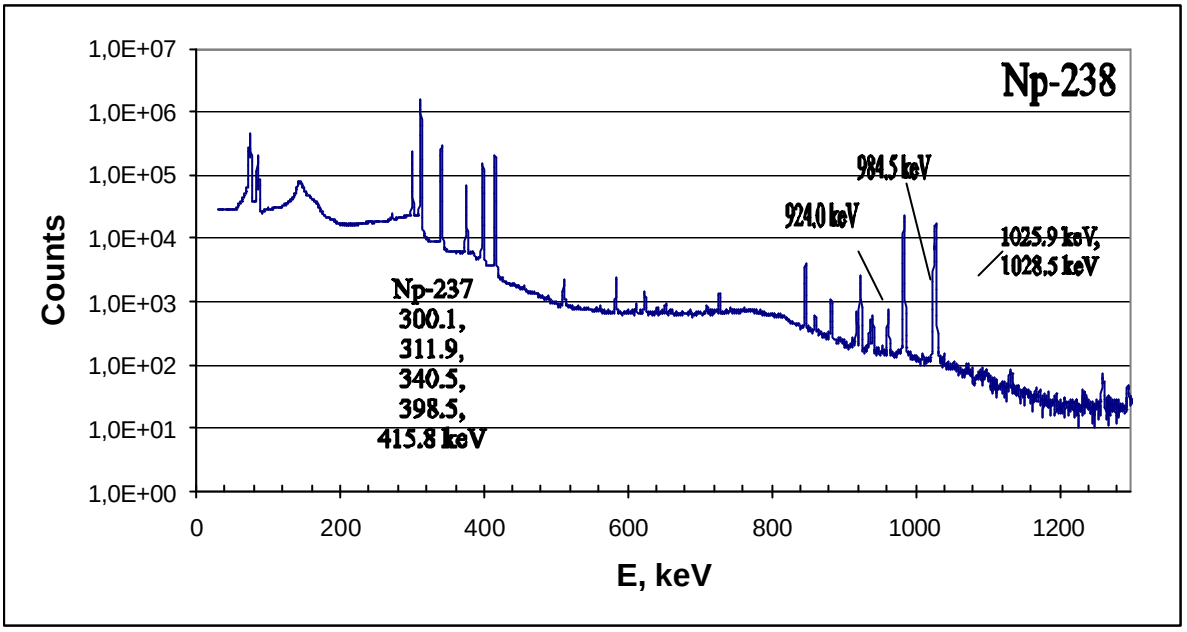

Fig. 44. Gamma-spectrum of ^{238}Np.

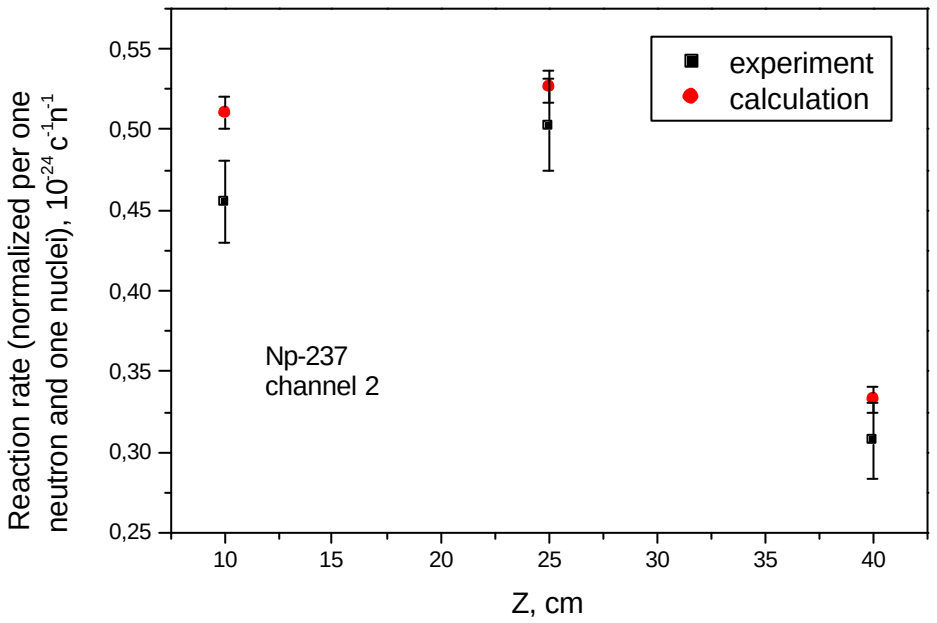

Fig. 45. Axial distribution of ^{237}Np(n, γ)^{238}Np reaction rates in experimental channel E2 (R = 10 cm).

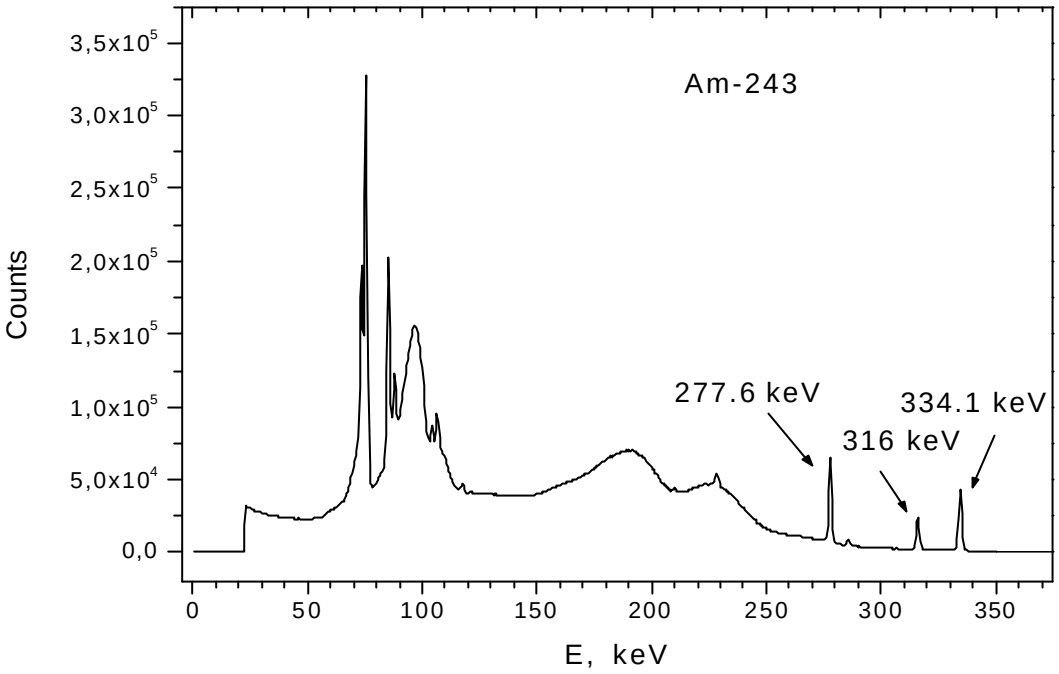

Fig. 46. Gamma-spectrum of ^{243}Am.

Analysis of the obtained results shows that calculated data agree well with experimental ones that confirms the applicability of MCNP – 4B code and evaluated nuclear data libraries for estimation of MA and LLFP transmutation rates in sub-critical systems with thermal neutron spectrum for which radiation capture reaction rates are well known.

7. Conclusion

A principal possibility of low energy accelerators and neutron generators application for investigations in the field of physics of multiplying system, driven by high energy (E_p ~ 0.6 – 2.0 GeV) particles accelerators has been shown. It results from a similarity of reactions' mechanism in the range of high and low energies where neutron energy spectrum is defined only by excitation energy of residual nucleus and practically does not depend upon energy of primary particle. Development of nucleon-meson cascade in neutron-producing targets irradiated by high energy protons comes finally to the stage when main part of neutrons escaping from targets have energies in the range of 15-20 MeV. Energy distribution of leakage neutrons in this energy range depends weakly upon both target (Pb, U, Ta, Bi…) material and energy of primary beam.

Just this statement became a basis for setting up the facility YALINA with thermal neutron spectrum, consisting of sub-critical blanket (k_{eff} < 0.98), neutron – producing lead target located at the core center and high intensity neutron generator NG-12-1 with neutron (E_n ~ 13-15 MeV) yield about $1.5 \cdot 10^{12}$ n/s. A distinctive feature of the created facility is possibility to vary core configuration for carrying out the experiments by sub-criticality levels up to $k_{eff} \leq 0.98$, application of different neutron external sources [^{252}Cf; d(d,n)^{3}He; d(T,n)^{4}He] with its' various locations relative to the core center.

Pulse mode of deuterium ions accelerator operation that allows to generate neutron pulses with duration 0.5 μs - 100 μs and repetition frequency 1 Hz - 10 KHz provides extended possibilities for the investigation of dynamics of multiplying media, development of the methods of sub-criticality level monitoring, working out the theoretical approach for description the peculiarities of neutron fields formation in deeply sub-critical systems.

Comparison of the results of experimental measurements of spatial distributions of reaction rates on ^{129}I, ^{237}Np, ^{243}Am nuclei and threshold reaction rates with those of calculation performed with application of MCNP-4B code and different libraries of evaluated nuclear data has shown fairly good agreement for different neutron sources, however for some reactions (Ti(n,p), Al(n,p)…) the discrepancy is observed that requires further analysis.

Measurements of deep sub-criticality and monitoring of neutron spectrum allow to investigate the effects of coupling of neutron-producing target and blanket.

A method of neutron spectrum determination in the core has been developed based on measurement of threshold (n,xnyp) reactions rates. In contrast to many known approaches it does not demand the knowledge of reference neutron spectrum.

Comparison of the results obtained by MCNP-4B code calculation with experimental ones have demonstrated that proposed approach may be of special interest for determination of neutron and proton spectra at sub-critical systems driven by high energy particles and will be used by realization of experimental program at SAD facility (Dubna, Russia).

One of the main parameters of sub-critical multiplying systems with external neutron sources is multiplication factor defining nuclear safety of the system. Application of the methods of k_{eff} measurements worked out for critical systems requires its' modification with taking into account all the peculiarities of formation of spatial, energy and time distributions of neutrons. For deep sub-criticality levels a deviation of time behavior of neutron flux from dependence predicted by point kinetics model is observed indicating that pulse neutron source method requires some modification for sub-criticality measurements.

In this connection more correct methods of sub-criticality measurement are those based on statistical approach (Sjöstrand method, source jerk method), and methods based on noise analysis. Combination of these methods allows to carry out with sufficient accuracy the experimental estimation of different kinetics parameters of sub-critical systems such as β_{eff}, Λ and ρ.

Further investigations in the field of ADS-technology at the NAS of Belarus will be performed on the basis facility YALINA-B consisting of sub-critical cascade reactor system driven by neutron generator NG-12-1. Distinguishing feature of such a nuclear system is that core consists of booster zone, where due to usage of highly enriched metallic and dioxide uranium fuel fast neutrons flux is formed and of thermal neutron spectrum zone. These zones are coupled each other by one-directional way of coupling due to the intermediate zone (thermal neutron absorber zone) where thermal neutrons escaping from thermal zone are absorbed. Such peculiarity of the core structure allows essentially increase power of the external neutron source, to generate fission pulses being many times shorter and intensive than those at traditional reactor systems, to carry out the experiments for study of the peculiarities of nuclear waste transmutation in conditions of fast and thermal neutron spectra and kinetics investigation of such systems by pulse mode of external neutron source (neutron generator) operation. Program of the experimental investigation includes development of methods of sub-criticality level monitoring, measurement of long-lived fission products and minor-actinides transmutation rates, study of sub-critical systems dynamics, measurements of spectral indices etc. Experimental data obtained at these facilities are important from the point of view of codes and nuclear data libraries validation, for sub-critical systems

calculation, for investigation of kinetics peculiarities of systems with external neutron sources etc. Simulation of booster sub-critical system neutronics based on Monte-Carlo method have shown that neutron energy spectrum in the booster zone, as well as neutron life time, time neutron flux response are very close to those obtained at SAD facility, consisting of sub-critical blanket with MOX fuel driven by high energy proton (Ep = 660 MeV) accelerator (JINR, Dubna, Russia).

The facilities YALINA and YALINA-B are very flexible sets up to study the physics of multiplying media with thermal and fast neutron spectrum at different sub-criticality levels, in wide range of various configurations (geometry, composition) and with different types of external neutron sources (^{252}Cf, D (d,n) ^{3}He, D (T,n) ^{4}He). These experimental facilities allow to obtain valuable data in the following fields:

- measurements of transmutation rates of fission products and minor actinides,
- investigation of spatial kinetics of sub-critical systems with external neutron sources,
- validation of experimental techniques for, e.g., sub-criticality monitoring, neutron spectra measurement, etc;
- investigation of dynamics characteristics of the sub-critical systems with external neutron sources operating in pulse mode.

References

[1] C.D. Bowman, Accelerator Driven Systems in Nuclear Energy. Role and Technical Approach: Report ADNA/97-013. ADNA Corporation/ Los Alamos.- New Mexico, 1997.

[2] V.I. Subbotin, Accelerators Promise to make Nuclear Energy Safer, Report at 85-th Session of JINR Scientific Council, 15 January 1999.– Dubna, (Preprint/ JINR; P1-99-97), p.24. (In Russian).

[3] R.G. Vasilkov, V.I. Goldanskiy, V.L. Gelepov, V.P. Dmitriyevskiy, Electronuclear Method of Neutron Generation, Atomic Energy, 1970.–V.29, N 3. –P.151 – 158. (In Russian)

[4] C. Rubbia, J.O. Rubio, S Buono et al., CERN – group. Conceptual Design of a Fast Neutron Operated High Power Energy Amplifier, Accelerator Driven Systems: Energy Generation and Transmutation of Nuclear Waste: Status Report/ IAEA-TECDOC-985.–Vienna, 1997, P. 187 – 312.

[5] M. Salvatores, M. Martini, I Slessarev. et al., MUSE-1: a First Experiment at MASURCA to Validate Physics of Sub-critical Multiplying Systems Relevant to ADS, IAEA-Techdoc-985.– Vienna, 1997, P. 430 - 436.

[6] S Chigrinov., H. Kiyavitskaya, Yu. Fokov et. al., The Research on Accelerator Driven Systems at the NAS of Belarus, IAEA –TM-25032, TWG-FR/108.– 49.- Vienna, 2002.

[7] ISTC Project 2267, Construction of the Subcritical Assembly with Combined Neutron Spectra Driven by Proton Accelerator at Proton's Energy 660 MeV for Experiments on Long Lived Fission Products and Minor Actinides, Project Manager - Shvetsov Valeri N. JINR, Dubna, Russia.

[8] S. Monti, First Panel Meeting on Evaluation of AIMA Preliminary Conceptual Design Studies of SC-Cyclotron for the TRADE Experiment, Presentation of the TRADE Project, 21 February 2002

Y. Kadi, A. Herrera-Martínez (CERN), L. Picardi, S. Monti (ENEA), M. Salvatores, The TRADE Experiment: Shielding of the Beam Transport Line, (CEA) - 10th International Conference on Radiation Shielding/13 ANS Radiation Protection and Shielding Division Topical Meeting, Funchal, Madeira, Portugal, May 9-14, 2004

[9] A.N. Kalinovskiy, N.V. Mokhov, Yu. P. Nikitin, Transport of High Energy Particles through a Matter, Moscow, Energoatomizdat, 1985, p. 248 (In Russian).

[10] K. Gudima, S. Mashnik, V.Toneev, Cascade-Exciton Model of Nuclear Reactions, Nucl. Phys., 1983, A401, P.329-361.

[11] K. Gudima, V.Toneev, Cascade-Exciton Model of Nuclear Reactions, Dubna, 1976, P/ 22 (Preprint / JINR; E4-9489).

[12] F.E. Bertrand, R.W. Peelle, Complete Hydrogen and Helium Particle Spectra from 30- to 60- MeV Proton Bombardment of Nuclei with A=12 to 209 and Comparison with the Intranuclear Cascade Model, Phys. Rev.,1973, V. C8,- P. 1045-1064.

[13] J. Franz, P. Koncs, E. Rossle et. al., Neutron-Induced Production of Protons, Deuterons and Tritons on Cupper and Bismuth, Nucl. Phys., 1990, V. A510, P. 774 - 802.

[14] R.E. Prael, H. Lichtenstein, User Guide to LSC: the LAHET Code System: Report LAUR-89-3014, Los Alamos National Laboratory, 1989.

[15] R.R. Fullwood, J.A. Cramer, R.A. Haarman et. al., Neutron Production by Medium Energy Protons on Heavy Metal Targets: Report LA-4789 UC-34, Los Alamos, New Mexico, 1972.

[16] H.Takada, S. Meigo, T. Sasa et. al., Present Status of Integral Spallation Experiments in JAERI / Accelerator Driven Systems: Energy Generation and Transmutation of Nuclear Waste: Status Report/ IAEA-TECDOC-985, Vienna, 1997, P. 187 – 312.

[17] S.E. Chigrinov, H.I. Kiyavitskaya, A.M. Khilmanovich et. al., Experimental Research of the Transmutation of Long - Lived Fission Products and Minor – Actinides in a Sub-critical Assembly Driven by a Neutron Generator, In Proc. ADTTA'96-Conf.–Kalmar, Sweden, 1996, P.737-744.

[18] V.S. Barashenkov, V.S. Buttsev, S.E. Chigrinov et.al., Fast Sub-Critical Assembly with MOX Fuel for Research on Nuclear Waste Transmutation, Journal of Vesti of NAS of Belarus, Ser. Physical – Technical Sciences, 2001, # 3, P.150-153. (In Russian).

[19] J.C. Astegiano, M. Daval, L. Martin et.al., Status of Fast reactors and ADS Programs in France in 2001, Review of National Programs on Fast Reactors and Accelerator Driven Systems (ADS), Karlsruhe, Germany, 22 – 26 April 2002 / IAEA –TM -25032, TWG-FR/108.– 2002.

[20] S.F. Boulyga, V.G. Goulo, I.V. Zhouk et. al., Neutron Generator NG-12-1 as a Basic Installation to Perform Researches at Neutron Center of the National Academy of Sciences of Belarus, (Preprint IRPCP- 21), Minsk, 1998, p.36. (In Russian).

[21] G.J Bell, S Glasstone, Nuclear Reactor Theory. (1970).

[22] N.G. Sjöstrand, Arkiv för Fysik, 11, 13 (1956).

[23] T. Gozani, Nukleonik, 4 (1962).

[24] F.S. Drozdov, A.S.Rychov, Determination of Negative Reactivity by Source Jerk Method, Atomic Energy, V.80, #1, 1969, P.74-75 (in Russian).

[25] J.F. Briesmeister, MCNP – A General Purpose N-Particle Transport Code, Version 4B: Report LA-12625-M/ Los Alamos National Laboratory, 1997.

[26] V.A. Naumov, I.E. Roubin,N.M. Dnieprovskaya, B.A. Litvinenko, N.A. Tetereva, Code KRATER for Calculation of Neutron – Physical Characteristics of Thermal Nuclear Reactors, Minsk, 1996, Preprint of NAS of Belarus, Institute of Power Engineering Problems, IPEP-14, p.39, (In Russian).

[27] B.A. Martsinkevich, A.M. Khilmanovich, S.V. Korneev, I.L. Rakhno, S.E. Chigrinov, M.I. Krivopustov, A.N. Sosnin, etc. Unfolding of Fast Neutron Spectra in Wide Energy Range (up to 200 MeV) at Sub-Critical Uranium-Lead Assembly of Electronuclear System, (Energy Plus Transmutation), Preprint P-2002-65, Dubna, Russia, 2002, p.20.